

## RESEARCH ARTICLE

# Risk assessment and spread of the potentially invasive *Ceratitis rosa* Karsch and *Ceratitis quilicci* De Meyer, Mwatawala & Virgilio sp. Nov. using life-cycle simulation models: Implications for phytosanitary measures and management



**Chrysantus Mbi Tanga<sup>1\*</sup>, Fathiya Mbarak Khamis<sup>1</sup>, Henri E. Z. Tonnang<sup>1,2</sup>, Ivan Rwomushana<sup>1</sup>, Gladys Mosomtai<sup>1</sup>, Samira A. Mohamed<sup>1</sup>, Sunday Ekesi<sup>1</sup>**

**1** International Centre of Insect Physiology and Ecology (ICIPE), GPO, Nairobi, Kenya, **2** International Maize and Wheat Improvement Centre (CIMMYT), ICRAF House, United Nations Avenue, Gigiri, Nairobi, Kenya

\* [ctanga@icipe.org](mailto:ctanga@icipe.org)

## OPEN ACCESS

**Citation:** Tanga CM, Khamis FM, Tonnang HEZ, Rwomushana I, Mosomtai G, Mohamed SA, et al. (2018) Risk assessment and spread of the potentially invasive *Ceratitis rosa* Karsch and *Ceratitis quilicci* De Meyer, Mwatawala & Virgilio sp. Nov. using life-cycle simulation models: Implications for phytosanitary measures and management. PLoS ONE 13(1): e0189138. <https://doi.org/10.1371/journal.pone.0189138>

**Editor:** Nikos T. Papadopoulos, University of Thessaly School of Agricultural Sciences, GREECE

**Received:** April 5, 2017

**Accepted:** November 20, 2017

**Published:** January 5, 2018

**Copyright:** © 2018 Tanga et al. This is an open access article distributed under the terms of the [Creative Commons Attribution License](#), which permits unrestricted use, distribution, and reproduction in any medium, provided the original author and source are credited.

**Data Availability Statement:** All relevant data are available from PANGAEA (<https://doi.pangaea.de/10.1594/PANGAEA.880370>).

**Funding:** This research was financially supported by the International Atomic Energy Agency (IAEA), through the CRP on “Resolution of Cryptic Species Complexes of Tephritid Pests to Overcome Constraints to SIT Application and International

## Abstract

Integrative taxonomy has resolved the species status of the potentially invasive *Ceratitis rosa* Karsch into two separate species with distinct ecological requirements: *C. rosa* “low-land type” and the newly described species *Ceratitis quilicci* De Meyer, Mwatawala & Virgilio sp. nov. “highland type”. Both species are tephritid pests threatening the production of horticultural crops in Africa and beyond. Studies were carried out by constructing thermal reaction norms for each life stage of both species at constant and fluctuating temperatures. Non-linear functions were fitted to continuously model species development, mortality, longevity and oviposition to establish phenology models that were stochastically simulated to estimate the life table parameters of each species. For spatial analysis of pest risk, three generic risk indices were visualized using the advanced Insect Life Cycle Modeling software. The study revealed that the highest fecundity, intrinsic rate of natural increase and net reproductive rate for *C. rosa* and *C. quilicci* was at 25 and 30°C, respectively. The resulting model successfully fits the known distribution of *C. rosa* and *C. quilicci* in Africa and the two Indian Ocean islands of La Réunion and Mauritius. Globally, the model highlights the substantial invasion risk posed by *C. rosa* and *C. quilicci* to cropping regions in the Americas, Australia, India, China, Southeast Asia, Europe, and West and Central Africa. However, the proportion of the regions predicted to be climatically suitable for both pests is narrower for *C. rosa* in comparison with *C. quilicci*, suggesting that *C. quilicci* will be more tolerant to a wider range of climatic conditions than *C. rosa*. This implies that these pests are of significant concern to biosecurity agencies in the uninvaded regions. Therefore, these findings provide important information to enhance monitoring/surveillance and designing pest management strategies to limit the spread and reduce their impact in the invaded range.

Trade, and EU-IBCARP Fruit Fly Project (DCI-FOOD/2014/346-739) through the International Centre of Insect Physiology and Ecology (icipe). We also gratefully acknowledge the icipe core funding provided by UK Aid from the Government of the United Kingdom; Swedish International Development Cooperation Agency (Sida); the Swiss Agency for Development and Cooperation (SDC); Federal Ministry for Economic Cooperation and Development (BMZ), Germany, and the Kenyan Government. The views expressed herein do not necessarily reflect the official opinion of the donors.

**Competing interests:** The authors have declared that no competing interests exist.

## Introduction

Temperature has a strong and direct effect on fruit fly development, reproduction and survival [1,2,3]. Global climate change and variability in temperature has also been attributed to the abundance, distribution and high infestation of fruit flies in different agro-ecological zones [4–6,1,7–9,3]. Temperature influences tephritid fruit fly population growth rates, increase in the number of generations, extension of the development season, changes in geographical distribution, crop-pest synchrony and interspecies interactions [1,10,7–9,3]. Estimating the relationship between temperature and development rate, survival and reproduction is thus important for predicting areas most suitable for insect species establishment. Predicting the potential distribution of fruitfly pests within the context of global climate variability and in particular temperature increase could help governments and growers adapt to changes in pest population by developing and equipping farmers with adequate pest management tools to reduce crop losses [11,10].

Changes in pest distribution and abundance in many agricultural systems have been predicted using various models [12,13]. These models are largely analytical tools that have been used to determine the risks associated with the behavior of agricultural pests under varying climatic scenarios [14,15]. Two distinct modeling approaches have been used for the evaluation, understanding, and prediction, of the dynamics of insect populations in agroecosystems and assessments of phytosanitary risks [16,15]. The first approach is the inductive method utilized to fit biologically relevant climatic stress functions to define species range limits. This approach matches the climate where an organism is normally found within a region to where it has not yet been reported using long-term meteorological data [40–44]. The second is the deductive method, which is used to define parameter values based on direct experimental observations of species responses to experimentally determined climatic factors or to phenological observations (process-based climate response models) [16]. It describes the basic physiological principles of the growth and development of a target insect species. These principles include development time, survival and reproduction [21–22]. This approach uses detailed laboratory experiments that produce life-table parameters and allows the simulation of populations according to real or interpolated data for a given region and time [24]. Although linear degree-day models have long been accepted as a basis for building phenology and population dynamics models [25–27], the nonlinearities at high and low temperatures have made them poor predictors of insect development. Due to nonlinearity at the high and low temperatures, non-linear models have been developed [28–30] that includes stochastic functions to account for variability in development times among individuals within a population [31,32]. Development of such phenology models requires knowledge of lower and upper developmental thresholds as well as data on development for each life stage of the pest [33,23].

In Africa, horticulture is undoubtedly one of the most attractive agricultural sub-sectors because it offers excellent opportunities for food and nutritional security, employment especially for youths and women, agro-processing needs, and also generates much-needed cash income for rural households. Hence, an improvement in horticultural productivity is viewed as a major economic development strategy for many sub-Saharan African (SSA) countries and beyond [34–36]. However, tephritid fruit flies afflict fruit and vegetable production and are recognized globally as the most important threat to horticulture, which limits the potential economic and social benefits of this activity [37–39]. Without control, direct damage by fruit fly species has been reported to range between 0–80% depending on the fruit or vegetable variety, location and season [40–47]. In addition to direct losses, indirect losses are associated with quarantine restrictions imposed by the importing countries to prevent entry and establishment of fruit fly pests [36,48]. The Natal fruit fly, *Ceratitis rosa* Karsch, is recognized as one of the

most economically important tephritid fruit fly pests in Africa attacking over 90 cultivated host plants [49,50]. *Ceratitis rosa* is largely restricted to eastern and southern Africa, but has successfully invaded the Indian Ocean islands of La Réunion and Mauritius, where it has been reported to out-compete the introduced *C. capitata* (Weidemann) and the native *Ceratitis catoirii* Guérin-Mèneville [17–21, 23–25, 51–57].

This work focused on *C. rosa*, which was originally thought to be restricted to the coastal region of Kenya [50] until 2001, when Copeland and Wharton [58] reported the first occurrence in the central highlands. Barr et al. [59] then conducted molecular studies on the two populations and suggested the possibility of two forms of *C. rosa*. Additional studies by Virgilio et al. [60] later confirmed the observation that the two populations of *C. rosa* in Kenya were actually made up of two distinct genotypic clusters identified as R1 and R2 [60–62,3] with largely overlapping geographic ranges. Also, through funding received from the International Atomic Energy Agency (IAEA) Coordinated Research Program (CRP) entitled “Resolution of Cryptic Species Complexes of Tephritid Pests to Overcome Constraints to SIT Application and International Trade”, an integrative approach to resolve the species status within the *Ceratitis* FAR (*Ceratitis fasciventris*, *Ceratitis anonae*, *Ceratitis rosa*) cryptic species complex using larval and adult morphology, wing morphometrics, cuticular hydrocarbons, pheromones, microsatellites, developmental physiology, geographical distribution, sexual compatibility, behavioural and chemoecological studies was conducted [61–63]. The studies concluded that the two *C. rosa* types represented two separate species with different ecological requirements: *C. rosa*, which has been referred to as “R1”, “the hot type” or “lowland type”, and *C. quilicii* sp. nov., referred to as “R2”, “the cold type” or “highland type”) [61,64]. Based on this new nomenclature, known museum specimens of *C. rosa* were revisited and taxonomically classified into *C. rosa* and *C. quilicii*. It is important to note that samples from many localities have not yet been assigned, as such the full distributional range of *C. rosa* and *C. quilicii* remains unknown (M. De Meyer, personal communication).

Previous studies on *C. rosa* revealed that no development occurred at low temperatures (< 15°C) but development rate increased with temperature up to an optimal temperature range of 27.9–31.4°C [65,1,3]. Beyond the optimal level, development rates decreased, dropping sharply as temperature approached the thermal limits of development and survival [1,3]. The studies by Tanga et al. [3] clearly demonstrate and support the existence of two genetically distinct populations of *C. rosa* (*Ceratitis rosa* Karsch and *Ceratitis quilicii* De Meyer, Mwatawala & Virgilio sp. Nov.) that are divergent in their physiological response to temperature with potential consequent implications in the invasion dynamics of these pests, there is a general lack of information on temperature-driven phenology models for these species, which include a set of functions describing temperature-dependency to determine the pests’ life history to forecast their development in Africa and beyond, which would be useful in the development of risk maps. This study was therefore designed to develop temperature-dependent population growth model for *C. rosa* and the newly identified species *C. quilicii*, and to assess their risk of spread in various agro-ecological zones in Kenya, Africa and globally using life-cycle simulation models: The findings on potential distribution, spread and impacts of these potentially invasive species may inform geographically-targeted policies in order to prevent new invasions and manage existing ones in Africa and beyond.

## Materials and methods

### Ethical statement

This study was not undertaken in national park or any protected areas. It was carried out in laboratory and open field screen houses using host species: guava (*Psidium guajava* L.) and

mango (*Mangifera indica* L.) and potentially invasive tephritid fruit fly species (*C. rosa* and *C. quilicci*). No specific permission was required for these experiments or collections due to the studies not involving endangered or protected species. This article does not contain any studies with human participants or animals performed by any of the authors.

### Fruit fly cultures

The wild populations of *C. rosa* and *C. quilicci* from Kenya were reared from infested fallen guava fruits collected at Kibarani, Msambweni district (S 04°19'62.8"; E 039°32'41.1"; 34 m a. s. l), and from infested mango fruits collected at Kithoka, Imenti North district (N 00°05'58.9"; E 037°40'39.5"; 1,425 m a. s. l), respectively. Stock cultures of the wild fruit fly populations from infested fruits were obtained following the methodology described by Rwmushana et al. [66]. The larvae of the two populations from the different host fruits were subsequently transferred into carrot-based artificial diet [67] after 2–3 generations on their natural hosts. Thereafter, *C. rosa* and *C. quilicci* populations were reared on artificial diets for 3–4 generations before commencement of the experiments. The identity of both colonies were confirmed using morphological characters of the adult males as outlined in De Meyer et al. [61]. The *C. rosa* colony was kept at 28 ± 1 °C, 50 ± 8% RH and photoperiod of L12: D12, while the *C. quilicci* colony was kept at 23 ± 1 °C, 65 ± 5% RH and photoperiod of L12: D12. Portable digital thermo-hygrometers were placed inside each of the rearing rooms of both fruit fly species to monitor temperature and relative humidity. To maintain the genetic vigour of the insects, about 300–500 new individuals collected from the same districts described above for each species were introduced into the respective colonies every six months. Both colonies were maintained at the Animal Rearing and Containment Unit (ARCU) of the International Centre of Insect Physiology and Ecology (icipe), Nairobi, Kenya.

### Egg collection

Newly emerged adults of *C. rosa* and *C. quilicci* were held separately in well ventilated transparent Perspex rearing cages (30 cm length x 30 cm width x 30 cm height). Adult flies were fed a diet consisting of 3 parts sugar and 1 part enzymatic yeast hydrolysate ultrapure (USB Corporation, Cleveland, OH). Water was also provided on pumice granules. The eggs of each fruit fly species were collected by offering them an oviposition substrate, which consisted of mango fruit domes (fruit skin that had the seed and pulp scooped out). The fruit domes were pierced with entomological pins (0.8 mm diameter) to facilitate oviposition by females. Freshly laid eggs were collected within a uniform time interval of 1 h after oviposition using a moistened fine camel's hair brush.

### Effect of temperature on development and survival of eggs, larvae and pupae of *C. rosa* and *C. quilicci*

The experiments were conducted in thermostatically controlled environmental chambers (MIR-554-PE, Sanyo/Panasonic cooled incubators, Japan) set at seven constant temperatures of 10, 15, 20, 25, 30, 33 and 35 °C (± 0.03 °C), 65 ± 5% RH and 12:12 L:D photoperiod to assess the effects of temperature on the development and survival of eggs, larvae, pupae and adults.

**Egg.** One hundred (100) eggs (1 h old) were randomly selected using a fine camel's hair brush, counted and carefully lined on moistened sterilized black cloth, which were thereafter placed on top of ≈ 60 g of artificial larval diet inside a Petri dish. The Petri dishes were immediately transferred into the seven controlled environmental chambers. The eggs were observed at 6-hourly intervals and the total number of eggs that had hatched at each temperature regime was recorded under a binocular microscope to determine the time and percentage egg hatch.

Egg development time and survival for each replicate were estimated. The experiments were replicated five times. The required temperatures inside the incubators were regularly monitored using standard thermo-hygrometers and experiments in which temperatures fluctuated more than  $\pm 0.03^{\circ}\text{C}$  were discarded and not included in the analysis.

**Larva.** One hundred neonate larvae ( $\sim 1$  h old) were randomly obtained from the fruit fly cultures and carefully transferred onto filter paper squares ( $2\text{ cm}^2$ ). The square filter paper containing neonate larvae were placed on top of a 150 g carrot-based artificial diet in 90-mm diameter Petri dishes. The Petri dishes containing the neonates were then placed in rectangular plastic rearing containers (21.5 cm x 15 cm) carrying a thin layer ( $\sim 0.5$  cm) of sterilized sand at the bottom for pupation, and then transferred to the thermostatically controlled environmental chambers. The lid of the plastic container (16.5 cm x 11 cm) was screened with cloth netting with a mesh size of 1.3 x 1.3 mm for ventilation. Larvae fed *ad libitum*, and mature larvae were allowed to freely leave the Petri dish into rectangular plastic containers for pupation. The sand was examined daily for newly formed pupae, and puparia were separated from the pupation medium by gentle sifting. Records of larval developmental durations were kept for the two fly populations at each temperature regime. The experiments were replicated five times.

**Pupa.** One hundred newly formed pupae ( $\sim 1$  h old) were randomly obtained from the fruit fly stock cultures and kept at the different rearing conditions described previously. Pupae used were placed in Petri dishes (8.6 cm diameter) and transferred into aerated transparent Perspex cages (30 cm x 30 cm x 30 cm) to allow for adult emergence. The cages were monitored on a daily basis for adult emergence, and pupal developmental time and survival were recorded. Those that did not emerge were observed for a longer time ( $\sim 1$  month) and recorded as dead in the absence of fly emergence. Number of adult flies that emerged and their sex were recorded daily. The experiments were replicated 5 times.

### Effect of temperature on fecundity, oviposition and longevity of adults

On the day of emergence, one female and one male ( $\sim 1$  h old) were paired and placed individually in aerated transparent Perspex cages (15 x 15 x 10 cm). Adult flies were provided with water on pumice granules and fed on a diet consisting of a mixture of enzymatic yeast hydrolysate powder and sugar in a ratio of 3:1. Thereafter, they were provided with oviposition substrates that consisted of a small mango dome placed over a sterile Petri dish (60 mm x 15 mm) lined with moistened filter paper. Each dome was pierced with an entomological pin to facilitate oviposition. Cotton wool soaked in water was placed in the rearing cages to maintain the relative humidity. The domes were exposed for 24 hr and thereafter the eggs were counted and the survival time of individual adult flies was also recorded. Eggs were collected daily using a moistened fine camel's hair brush and total number of eggs produced per day over the lifetime of each fly was determined. A total of 15 pairs of adult flies were observed at each tested temperature regime for each fruit fly population.

Similarly, an additional cohort of 100 freshly emerged adult females and 100 males ( $\sim 1$  h old) of each fruit fly population were kept in transparent Perspex cages (30 by 30 by 30 cm; length by width by height) at the different temperature regimes and their longevity and survival time were recorded separately for males and females.

### Field experiments under fluctuating temperatures

Life table experiments were carried out for the fruit fly species (*C. rosa* and *C. quilicci*) under natural fluctuating temperatures to evaluate if the data collected in the laboratory under constant temperatures provided realistic predictions for development and survival. The

experimental cages were maintained on table surfaces (324 cm length x 87 cm width x 76 cm height) in a shaded outdoor location at the *icipe* Duduville campus, Nairobi [S 01° 13' 14.6"; E 036° 53' 44.5"], 1612 m above sea level (a.s.l)], where they received ample light and air circulation but no direct sunlight. The edges of the tables as well as the feet on which the cages were placed were smeared with Tanglefoot® insect barrier paste (Tangle-trap; The Tanglefoot Company, Grand Rapids, MI) to prevent attack by predacious insect species. The table stands were also placed in containers filled with soapy water to further deter predatory insects from accessing the fruit flies in the cages. The water in the containers was replenished when necessary.

The protocol used was similar to that described above under constant temperatures. Freshly laid eggs (~1 h old) were collected from the rearing cages, counted and distributed in five replicates of 100 eggs each. The eggs were placed in the open air where they were observed daily and the developmental duration of each egg and the total number of eggs that hatched was recorded. For the larval development, 100 newly hatched larvae (~1 h old) were transferred individually with a camel hair brush into a 9-cm-diameter Petri dish containing artificial diet and placed in the open air where they were observed daily and developmental time recorded. The experiments were replicated 5 times. On the other hand, 100 newly developed puparia from the stock cultures (~1 h old) were also randomly selected and placed into Petri dishes before transferring into small transparent Perspex cages (20 length x 20 width x 20 cm heights), where they were observed for emergence. The experiments were replicated 5 times. Daily minimum and maximum temperature was recorded throughout the year at the experimental site using a HOBO UX100 Temp/RH Data Logger (Part # UX100-003).

### Model building and validation using Insect Life Cycle Modeling (ILCYM version 3.0)

The *C. rosa* and *C. quilicci* phenological models were built using Insect Life Cycle Modeling software (ILCYM version 3.0) [68,15]. The software has tools for building process-based population models for insect species. The model builder uses the same shape distribution approach combined with a rate summation and cohort up-dating for simulation of population dynamic models. ILCYM has several non-linear functions that describe the temperature-dependency of different processes in the life history of insects. These include the development time and its variation between individuals in a population, mortality in each immature life-stage, adult longevity (senescence), and reproduction frequencies of the adults according to temperature. The model builder, using its inbuilt statistical criteria, combined with knowledge on the biology of the species under investigation, facilitates the selection of the best fitting functions for describing these temperature-driven processes and then compiles the processes into a phenological model for each of the populations under investigation [69].

### Temperature-dependent process models and statistical analysis

The relationship between temperature-dependence of different processes in the *C. rosa* and *C. quilicci* life history and different temperature regimes were analyzed by various non-linear models, using the ILCYM software [69]. The statistical analysis implemented in this software selected the best-fitting model to quantify the effect of temperature on development time, mortality, senescence and reproduction according to inbuilt model selection criteria. These criteria were the Akaike's Information Criterion (AIC), which defines the goodness of an estimated statistical model, and the coefficient of determination,  $R^2$ , which explains how the models capture the variability within the data. A female ratio of 0.5 was assigned for all the temperature regimes that were studied.

## Modeling development time and distribution of *C. rosa* and *C. quilicci*

The cumulative probability distribution of *C. rosa* and *C. quilicci* development time under different temperatures were estimated and normalized. Frequency distributions for insect development time are usually skewed towards longer times and it is assumed that development times of insects at different temperatures are of the same shape. The log-transformed data were arranged into a frequency distribution and fitted to a logit model [22]. The fitted generalized linear models to the normalized development time were the logit model for the egg, larva and pupa with the mathematical expression given as

$$F(x) = \frac{1}{1 + \exp(-(a_i + b \ln x))}$$

Where  $F(x)$  is the probability to complete development at time  $x$ ,  $\ln x$  is the natural logarithm of the development days observed,  $a$  is the intercept corresponding to the temperature ( $i$ ) and  $b$  is the common slope of the regression model representing the dispersion of the development time in the life stages.

## Development rate

According to Khadioli et al. [70], temperature-dependent development of insects from one stage to another does not follow a linear relationship; as such they are usually less preferred for use in phenology models. Therefore, in describing the relationship between temperature and the development rate of the two fruit fly populations, ILCYM provides several non-linear functions and other models that have been used successfully for many insect species [68]. The development time  $d$  was used to calculate development rates. The temperature-dependent development rate of *C. rosa* and *C. quilicci* was best described by the Brière 1 model for all temperature regimes [3] and allowed for the estimation of the upper and lower developmental thresholds [30]. The Brière -1 model is given by the expression:

$$r(T) = aT(T - T_{min}) X \sqrt{T_{max} - T}$$

where,  $r$  is the developmental rate as a function of temperature ( $T$ ), and ' $a$ ' is an empirical constant. The following equation from Brière et al. [30] was used to calculate the optimum temperature:

$$T_{opt} = \frac{4T_{max} + 3T_{min} + \sqrt{16T_{max}^2 + 9T_{min}^2 - 16T_{min}T_{max}}}{10}$$

The mean values for  $T_{min}$ ,  $T_{opt}$  and  $T_{max}$  were determined for each life stage of each group of *C. rosa* and *C. quilicci* using the results generated by the developmental rate models. The choice of the best-fitting function in ILCYM was done using the  $R^2$  statistics or the AIC [71]. The lower development threshold which is defined as the temperature below which there is no measurable development was estimated by the linear regression.

$$r(T) = a + b.T$$

where  $r(T)$  is the development rate,  $a$  and  $b$  represent the intercept and the slope of the equation, respectively.

## Immature mortality

The mortality rate in the immature life stage was calculated from the relative frequency of cohort survivors. A polynomial mathematical expression was fitted to describe the relationship between the mortality rate and the temperature for each life stage. The equation is given below

where  $M(T)$  is the rate of mortality at temperature  $T$ ; and  $b_1, b_2, b_3$  are parameters to be estimated.

$$M(T) = \exp^{b_1 + b_2x + b_3x^2}$$

### Adult life span and aging

The mean survival time of the adult was determined for both sexes and the inverse of the survival time was plotted against temperature. A modified four parameter Stinner model [26] was fitted to determine the relationship between adult longevity rate of both the male and female adults and temperature. The mathematical expression of the model is given as

$$S(T) = \frac{C_1}{1 + e^{(k_1 + K_2 T)}} + \frac{C_2}{1 + e^{k_1 + k_2(T_0 - T)}}$$

where,  $S(T)$  is the senescence rate at temperature  $T(^{\circ}\text{C})$ ,  $C_1$  and  $C_2$  are maximum and minimum temperatures, respectively.  $T_0$  is the optimum temperature and  $K_1$  and  $K_2$  are constants.

### Temperature-dependent reproduction

For *C. rosa*, a polynomial regression was applied to determine the effect of the temperature on the total number of eggs laid per female during her entire life span. The expression of the model is given as

$$F(T) = b_1 + b_2.x + b_3.x^2$$

where  $F(T)$  is the total eggs per female.

A Gaussian equation [72] was applied to determine the effect of temperature on the total number of eggs laid per *C. quilicci* adult female fly. The expression of the model is:

$$f(T) = \frac{1}{1 + R_{max} \cdot e^{-a \left( \frac{T - T_{max}}{b} \right)^2}}$$

where,  $f(T)$  is the fecundity at temperature  $T(^{\circ}\text{C})$ ,  $R_{max}$  is the maximum fecundity,  $T_{max}$  is the temperature at which maximum fecundity occurs, and  $a$  and  $b$  are the fitted parameters representing intercept and slope of the equation, respectively.

An exponential model was fitted to describe the age-specific fecundity rate at each of the test temperatures. The cumulative oviposition rate was plotted against normalized female age expressed as ratio of age in days divided by mean survival time. Below is the formula of the exponential equation which was used for assessing the relative oviposition frequency of both fruit fly species:

$$y = 1 - e^{-(aX + bX^2 + cX^3)}$$

where,  $y$  is the cumulative oviposition frequency,  $X$  is the normalized age of female expressed as a ratio of age in days and mean survival time, and  $a$ ,  $b$  and  $c$  are the equation parameters.

### Life table parameters of *C. rosa* and *C. quilicci*

Using ‘stochastic simulation tool’ in ILCYM, the life table parameters i.e. gross reproductive rate (GRR), net reproductive rate ( $R_0$ ), mean generation time (T), intrinsic rate of natural increase ( $r_m$ ), finite rate of increase ( $\lambda$ ), and doubling time ( $D_t$ ) of *C. rosa* and *C. quilicci* were estimated based on the developed phenology model. The simulation method was based on the

rate summation and cohort updating approaches (i.e. random determination for the survival and development of each individual to the next stage) [21]. The simulations started with an initial number of 100 individuals from the egg stage for a given constant temperature regime and were performed over seven constant temperatures ranging from 10 to 35°C with 50 repetitions for each temperature. The estimated life table parameters were plotted against the respective temperatures and fitted to a quadratic equation.

$$L_p(T) = a + bT + cT^2$$

Where,  $L_p(T)$  represents the respective life table parameters (GRR,  $R_o$ , T,  $r_m$ ,  $\lambda$ ,  $D_t$ ) at temperature T (°C), and  $a$ ,  $b$  and  $c$  are the model parameters.

### Evaluation of the phenological models

The input data for the validation model were obtained from the experiment conducted outdoors using open field cages under fluctuating temperatures. Data obtained from the temperature and relative humidity data loggers showed that the minimum and maximum temperatures recorded during the experiment period (16<sup>th</sup> September 2014 to 28<sup>th</sup> December 2015) ranged between 9.14–16.68°C and 18.84–37.66°C, respectively. Experimental life table data points collected based on developmental duration, mortality, longevity and population growth parameters obtained from fluctuating temperature studies were used for validating the results of the model outputs produced from the laboratory constant temperatures experiments using stochastic simulation. ILCYM stochastically simulates a user-defined number of life tables, each with a user-defined number of individuals, through rate summation and random determination for survival of each individual, and development to the next stage. The output of the simulation is then presented in a graphical format. The Euclidian distance between the observed and simulated data points is provided to show the difference between the simulated and the observed data points. The closer the Euclidian distance value is to zero (0), the better the developed phenology model at constant temperature and results can be used to predict the species distribution and population abundance in natural field conditions under fluctuating temperatures.

### Climate data used in spatial analysis

The mean minimum and maximum temperature information collected during the outdoor experiment under fluctuating temperature were considered as current climatic conditions. For Kenya, a spatial resolution of 2.5 arc-min was used whereas 10.0 arc-min was applied for Africa. In predicting *C. rosa* and *C. quilicci* response to climate change, we down-scaled, bias-corrected and open source spatial database accessible at AFRICLIM (<http://www.york.ac.uk/environment/research/kite/resources/>) to project temperature changes. With validation of the predictive ability of the model, we projected the model worldwide to identify areas of potential distribution and possible invasion for each of the species. The simulation for the global prediction was carried out using the climate data obtained from WorldClim (<http://www.worldclim.org/>) and CCAFS (<http://www.ccafs-climate.org>) databases as described in Kroschel et al. [15]. The available down-scaled values of current temperature (mean daily minimum and maximum) in raster format were loaded and opened in Quantum Geographic Information System software (QGIS) [73].

### Potential population distribution and risk mapping of *C. rosa* and *C. quilicci*

The Insect Life Cycle Modeling software (ILCYM version 3.0) [15] was used to generate *C. rosa* and *C. quilicci* risk maps using the validated phenology model. Linked with GIS, the

model allows the simulation of pest risk indices. The indices used for mapping included establishment risk index (ERI), generation index (GI) and activity index (AI), which were produced from the obtained population growth parameters as described by Kroschel et al. [15]. The ERI identifies the area in which the pest may survive and become established and it is estimated based on a daily scale by the following expression:

$$ERI = \frac{\sum_{i=1}^{i=365} I_i}{I_I} * net - reproduction$$

Where,  $I_i$  is the interval of day  $i$  (with  $i = 1, 2, 3, \dots, 365$ ) and the total number of intervals,  $I_I$ , is 365. The index is 1 when all the immature stages of *C. rosa* or *C. quilicci* survive throughout the year at varied proportions, with  $ERI < 1$  characterizing areas in which survival and establishment of the population is restricted to certain periods in the year.

The GI estimates the mean number of generations that may be produced within a given year, calculated by averaging sum of the estimated generation lengths in each Julian day as shown in the formula:

$$GI = \frac{\sum_{x=1}^{365} 365/T_x}{365}$$

where,  $T_x$  is the predicted generation length in days at Julian day  $x$  ( $x = 1, 2, 3, \dots, 365$ ). This implies that an increase in temperature will lead to an increase in the number of generations per year. But, in real life, extreme temperatures reduce fecundity and increase mortality, disrupting the finite rate of natural increase ( $\lambda$ ).

The AI is explicitly related to the finite rate of population increase of *C. rosa* and *C. quilicci* populations, which takes the whole life history of the pest into consideration. The index is calculated by taking a log of products of the estimated finite rates of natural increase for each Julian day as shown below:

$$AI = \log_{10} \prod_{x=1}^{365} \lambda_x$$

where,  $\lambda_x$  is the finite rate of increase at Julian day  $x$  ( $x = 1, 2, 3, \dots, 365$ ). Every increase of AI by 1 implies a 10-fold increase of the pest population [24].

Using the index interpolator (a sub-module of ILCYM), the compiled *C. rosa* and *C. quilicci* phenology, the Digital Elevation Model (DEM) obtained from the Shuttle Radar Topography Mission (SRTM), and the temperature data in text files, were imputed into ILCYM and the pest risk indices generated in American Standard Code for Information Interchange (ASCII) formats [74]. Obtained results were transferred into QGIS for analysis, visualization and interpretation.

## Statistical analysis and modeling tools

All analyses for developing the temperature-dependent phenology model were conducted using the ‘model builder’ tool in Insect Life Cycle Modelling (ILCYM) software, version 3.0 (International Potato Centre, Lima, Peru) [69]. The best fit model in each case was selected based on well-known goodness of fit indicators such as Akaike’s Information Criterion (AIC) [71] and coefficient of determination ( $R^2$ ) along with application of our expert knowledge on biology of *C. rosa* and to predict their life history under a range of environmental temperatures. We then used Analysis of Variance (ANOVA) and least significance difference (LSD) post-hoc tests at a significance level of  $P = 0.05$  for probability thresholds and hypothesis testing in all the regressions to determine which individual traits were governed by these factors.

## Results

### Temperature-dependent mortality rates of *C. rosa* and *C. quilicci*

The lethal time period when mortality reached 50% (LT 50) or 100% (LT 100) varied considerably between *C. quilicci* (Fig 1A and Table 1) and *C. rosa* (Fig 1B and Table 1) immature life stages (egg; larva and pupa). According to the model, *C. quilicci* had a lower LT100 threshold at 5.2, 4.8 and 5.9°C and an upper LT100 threshold at 35.2, 35.1 and 33.3°C for the eggs, larvae and pupae, respectively. For *C. rosa* the lower LT100 was observed at 10.4, 9.6 and 7.2°C, and an upper LT100 threshold at 37.6, 37.8 and 33.3°C for the eggs, larvae and pupae, respectively. The LT50 of *C. quilicci* was recorded at 25°C for eggs and larvae, while that of the pupae was 23.8°C. The LT50 of *C. rosa* was recorded at 23.6°C for the eggs and larvae, while that of the pupa was at 20°C.

### Adult reproduction and longevity of *C. rosa* and *C. quilicci*

The preoviposition, oviposition and postoviposition duration of both *C. rosa* and *C. quilicci* were inversely correlated with temperature (Table 2). The preoviposition, oviposition and post-oviposition durations were significantly different across the different temperature regimes for *C. rosa* and *C. quilicci*. At the same temperature, the pre-oviposition duration for *C. rosa* and *C. quilicci* was significantly different at 15°C, 20°C and 33°C, whereas it was

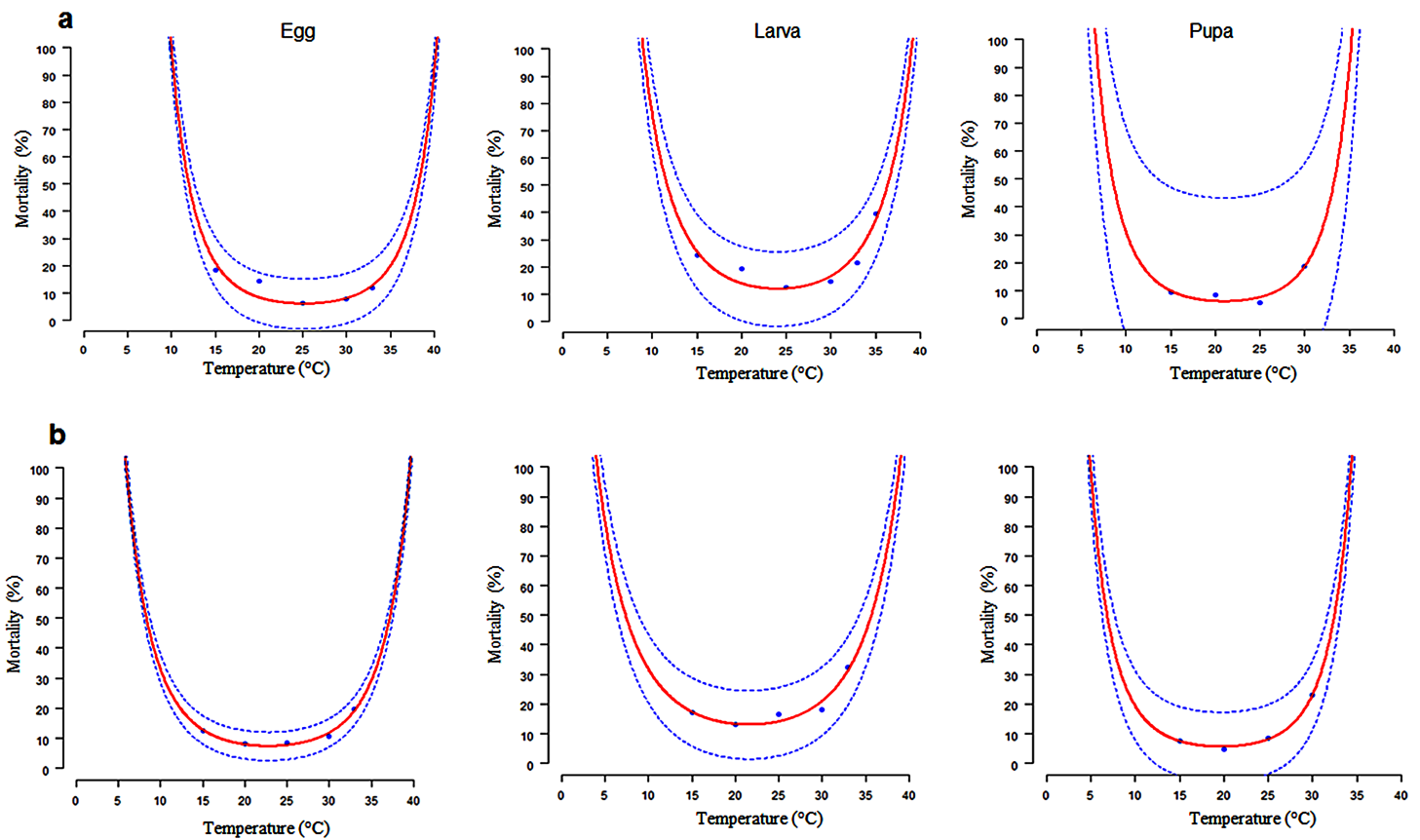


**Fig 1.** Temperature-dependent mortality rates of *C. rosa* (1a) and *C. quilicci* (1b) immature life stages (egg; larva and pupa) at six different constant temperatures. Fitted curves: Polynomial regression for all immature stages. The upper and lower 95% confidence intervals of the model are indicated. Markers are observed means, bars represent standard deviation.

<https://doi.org/10.1371/journal.pone.0189138.g001>

**Table 1. Estimated parameters (mean ± SE) of the exponential model:  $f(T) = \exp(b_1 + b_2.x + b_3.x^2)$ , fitted to mortality rate for eggs, larva and pupa stages of *Ceratitis rosa* and *Ceratitis quilicci*.**

	Parameters	Immature life stage		
		Eggs	Larva	Pupa
<i>C. rosa</i>	b1	10.271 ± 0.002	9.621 ± 0.0014	7.178 ± 0.0031
	b2	-0.909 ± 0.0235	-0.453 ± 0.0161	-0.570 ± 0.0332
	b3	0.019 ± 0.0006	0.009 ± 0.0005	0.014 ± 0.0012
	$r^2$	0.984	0.881	0.912
<i>C. quilicci</i>	b1	5.183 ± 0.0008	4.812 ± 0.0012	5.8716 ± 0.0560
	b2	-0.422 ± 0.0086	-0.290 ± 0.0140	0.3892 ± 0.0020
	b3	0.009 ± 0.0003	0.007 ± 0.0005	141.781 ± 0.0054
	$r^2$	0.973	0.936	0.912

<https://doi.org/10.1371/journal.pone.0189138.t001>

comparable at 25°C, 30°C and 35°C. The oviposition duration of *C. rosa* and *C. quilicci* was significantly different at 15°C, 20°C, 30°C and 35°C, but comparable at 25°C and 33°C. On the other hand, the post-oviposition duration of *C. rosa* and *C. quilicci* was significantly different at 25°C, 33°C and 35°C, while it was similar at 15°C, 20°C and 30°C for both fruit flies. However, there were significant interactions between the different temperature regimes investigated and fruit fly species with regards to pre-oviposition ( $F = 5.54$ ; d.f. = 5, 168;  $P = 9.45 \times 10^{-5}$ ), oviposition ( $F = 6.78$ ; d.f. = 5, 168;  $P = 8.8 \times 10^{-6}$ ) and post-oviposition duration ( $F = 4.09$ ; d.f. = 5, 168;  $P = 1.57 \times 10^{-3}$ ).

The mean number of eggs produced by *C. rosa* and *C. quilicci* throughout their entire life span was found to vary significantly across the different temperature regimes. Within the same temperature regime the lifetime fecundity of *C. rosa* and *C. quilicci* was found to vary significantly. Similarly, the interactions between the two fruit fly species and the temperature regimes were found to be highly significant for adult fecundity ( $F = 11.85$ ; d.f. = 5, 168;  $P = 7.97 \times 10^{-10}$ ). The lifetime fecundity per adult female of *C. rosa* was found to range between  $153.2 \pm 12.7$  eggs at 15°C to  $805.7 \pm 79.9$  at 30°C, while for *C. quilicci*, it ranged between  $118.5 \pm 8.9$  eggs at 35°C to  $617.1 \pm 39.6$  eggs at 25°C (Table 2). The effects of temperature on the fecundity of *C. rosa* was described by a second-order polynomial function ( $F = 13.98$ ; d.f. = 2, 5;  $P = 0.0302$ ) (Fig 2A and Table 3), while the cumulative proportion of eggs produced per female and normalized female age was described by a second-order modified exponential function (Fig 2B and Table 3). For *C. quilicci*, the effects of temperature on fecundity was described by a simple Gaussian function ( $F = 2.15$ ; d.f. = 2, 5;  $P = 0.3333$ ) (Fig 2C and Table 4), while the cumulative

**Table 2. Effect of different constant temperature on the pre-oviposition, oviposition, post-oviposition periods (days), fecundity and longevity of *Ceratitis rosa* and *Ceratitis quilicci*.**

Temp (°C)	Pre-oviposition		Oviposition		Post-oviposition		Fecundity	
	<i>C. rosa</i>	<i>C. quilicci</i>	<i>C. rosa</i>	<i>C. quilicci</i>	<i>C. rosa</i>	<i>C. quilicci</i>	<i>C. rosa</i>	<i>C. quilicci</i>
15	58.27±3.48 <sup>aB</sup>	43.27±2.86 <sup>aA</sup>	79.27±3.70 <sup>aB</sup>	92.87±4.09 <sup>aA</sup>	48.33±2.45 <sup>aA</sup>	55.33±5.51 <sup>aA</sup>	153.2±12.73 <sup>cB</sup>	242.13±19.42 <sup>dA</sup>
20	28.93±1.87 <sup>B</sup>	23.07±1.71 <sup>bA</sup>	67.27±1.91 <sup>bB</sup>	88.87±4.65 <sup>aA</sup>	17.87±1.34 <sup>bA</sup>	20.47±3.31 <sup>bA</sup>	297.87±28.61 <sup>bB</sup>	402.07±35.93 <sup>cA</sup>
25	14.53±1.20 <sup>cA</sup>	17.87±1.43 <sup>cA</sup>	52.13±3.19 <sup>cA</sup>	46.27±2.72 <sup>bB</sup>	12.53±1.19 <sup>cB</sup>	7.27±2.01 <sup>cA</sup>	776.07±43.19 <sup>bB</sup>	617.13±39.62 <sup>aA</sup>
30	12.47±1.16 <sup>cA</sup>	15.33±1.31 <sup>cdA</sup>	35.13±2.31 <sup>dB</sup>	28.67±2.21 <sup>cA</sup>	8.13±1.22 <sup>dA</sup>	5.47±1.16 <sup>cA</sup>	805.73±79.86 <sup>aA</sup>	523.67±35.16 <sup>bB</sup>
33	10.33±0.54 <sup>cB</sup>	12.07±0.58 <sup>dA</sup>	24.27±2.05 <sup>eA</sup>	21.73±1.55 <sup>cA</sup>	6.53±0.61 <sup>dB</sup>	3.67±1.22 <sup>cA</sup>	625.47±49.16 <sup>bB</sup>	393.27±20.83 <sup>cA</sup>
35	9.73±0.38 <sup>cA</sup>	11.07±0.69 <sup>dA</sup>	18.27±1.32 <sup>eB</sup>	12.73±0.92 <sup>dA</sup>	3.73±0.52 <sup>dB</sup>	2.27±0.82 <sup>cA</sup>	179.13±13.90 <sup>cB</sup>	118.47±8.90 <sup>aA</sup>

Means in the same column followed by the same upper case and in the same row followed by the same lower case letter are not significantly different [ANOVA and Student–Newman–Keul's (SNK) test,  $P < 0.05$ ].

<https://doi.org/10.1371/journal.pone.0189138.t002>

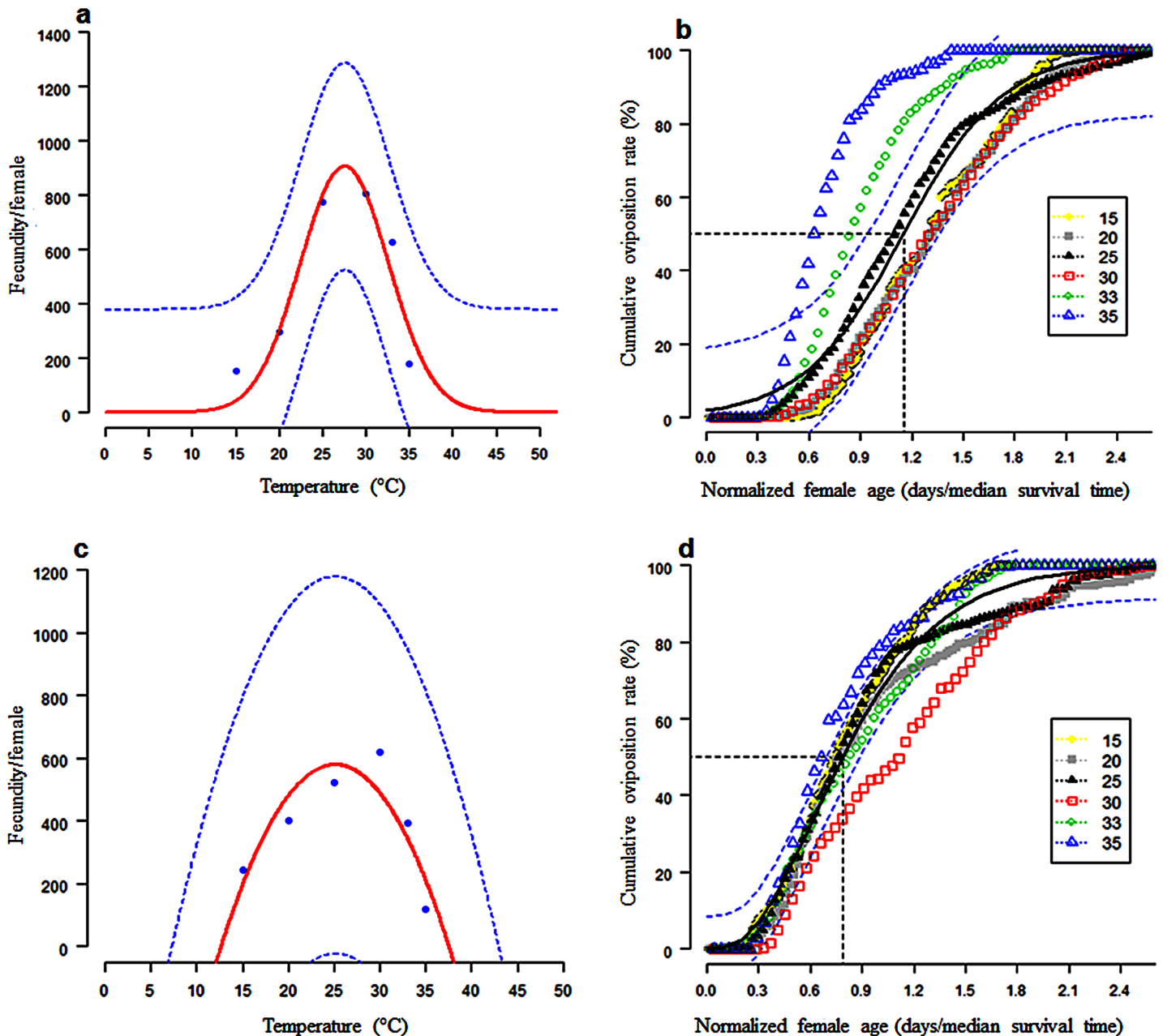


**Fig 2.** Temperature-dependent total egg production curve for *C. rosa* (fitted function: Polynomial model) and *C. quilicci* (fitted function: Guassian denominated function) (2a and 2c, respectively). Age-related oviposition rate for *C. rosa* (2b; fitted curve: Second-order polynomial function) and *C. quilicci* (2d; fitted curve: Gamma distribution function). The dots are observed data points at each of the test temperatures. The upper and lower 95% confidence intervals of the models are indicated. Age of the females at 50% oviposition is indicated.

<https://doi.org/10.1371/journal.pone.0189138.g002>

proportion of eggs produced per female and normalized female age was well described by the gamma-function (Fig 2D and Table 4).

The average longevity of adult females of *C. rosa* ( $F = 237.5$ ; d.f. = 5, 84;  $P = 2 \times 10^{-14}$ ) and *C. quilicci* ( $F = 202.9$ ; d.f. = 5, 84;  $P = 2 \times 10^{-16}$ ) were found to significantly decrease with increasing temperature (Fig 3A for *C. rosa* and Fig 3B for *C. quilicci*). The longevity of *C. rosa* was  $31.9 \pm 1.5$  days at  $35^{\circ}\text{C}$  and  $185.9 \pm 6.7$  days at  $15^{\circ}\text{C}$ , whereas that of *C. quilicci* was  $15.0 \pm 1.0$

**Table 3.** Relationship of the total eggs per *Ceratitis rosa* female with temperature (polynomial function), and age-related cumulative proportion of progeny produced (exponential function).

Response variable	Second-order polynomial function: $f(T) = \exp(b1 + b2.x + b3.x^2)$			
	b1	b2	b3	$r^2$
Total eggs/female	-7.851 (0.0019*)	1.064 (0.0258*)	-0.019 (0.0009*)	0.903
Second-order exponential modified function: $O(E) = 1/(1+\exp(a+bE))$				
	a	b		$r^2$
Proportion of progeny production	3.94859 (0.0933*)	-3.43037 (0.0778*)		0.9399

Numbers in parentheses are standard errors of estimates

\* $f(T)$ , fecundity at temperature T (°C).

<https://doi.org/10.1371/journal.pone.0189138.t003>

days at 35°C and  $199.4 \pm 10.0$  days at 15°C. Within the same temperature regime, the longevity of female *C. rosa* and *C. quilicci* was significantly different at 20°C, 33°C and 35°C, whereas it was comparable at 15°C, 25°C and 30°C. There was significant interaction between the adult fruit fly species and temperature regimes for longevity ( $F = 5.75$ ; d.f. = 5, 168;  $P = 6.35 \times 10^{-5}$ ). Male longevity was greater than that of females for *C. rosa* (Fig 3A) and *C. quilicci* (Fig 3B) at all temperature regimes investigated.

The exponential model gave a good fit to the observed mean senescence of both sexes of *C. rosa* (Fig 4A and Table 5) and *C. quilicci* (Fig 4B and Table 5).

### Life table parameters of *C. rosa* and *C. quilicci*

The models established were compiled in an overall phenology model for stochastic simulation of *C. rosa* and *C. quilicci* to generate all the life table parameters (Table 6). The intrinsic rate of natural increase ( $r_m$ ), the net reproductive rate ( $R_o$ ), the finite rate of increase ( $\lambda$ ), the mean generation time ( $I$ ) and doubling time ( $D$ ) were estimated for each temperature regime. The life-table parameters showed that *C. quilicci* and *C. rosa* populations can develop successfully within the temperature range of 15–35°C. The highest intrinsic rate of increase of *C. rosa* was  $0.19 \pm 2.7 \times 10^{-3}$  at 30°C, while that of *C. quilicci* was  $0.14 \pm 1.1 \times 10^{-3}$  at 25°C. The net reproductive rate  $R_o$  differed significantly among temperatures with the highest at 30°C for *C. rosa* ( $189.17 \pm 5.49$ ) and 25°C for *C. quilicci* ( $100.72 \pm 4.58$ ) and. The lowest values of  $r_m$  and  $R_o$  for *C. rosa* and *C. quilicci* were recorded at 15°C and 35°C. Maximum values of finite rate of increase ( $\lambda$ ) for *C. rosa* and *C. quilicci* recorded at 30°C. Values estimated for ‘T’ showed that the mean length of generations decreased with increase in temperatures from  $84.57 \pm 0.58$  days at 15°C to  $35.47 \pm 0.28$  at 33°C for *C. rosa*, where as that of *C. quilicci* varied from  $83.70 \pm 0.57$  days at 15°C

**Table 4.** Relationship of the total eggs per *Ceratitis quilicci* female with temperature (Guassian denominated function), and age-related cumulative proportion of progeny produced (Gamma function).

Response variable	Gaussian denominated function: $f(T) = y0 + a \cdot \exp(-0.5((x - x0)/b)^2)$				
	y0	a	b	x0	$r^2$
Total eggs/female	-41393.36 (3.8096*)	41971.86 (29.3741*)	74.63 (19.0522*)	25.126 (7.8725*)	0.7632
Gamma function: $O(E) = \text{pgamma}(E, a, b)$					
Proportion of progeny production		a	b		$r^2$
		3.404 (0.0686*)	3.906 (0.08242*)		0.9823

Numbers in parentheses are standard errors of estimates

\* $f(T)$ , fecundity at temperature T (°C).

<https://doi.org/10.1371/journal.pone.0189138.t004>

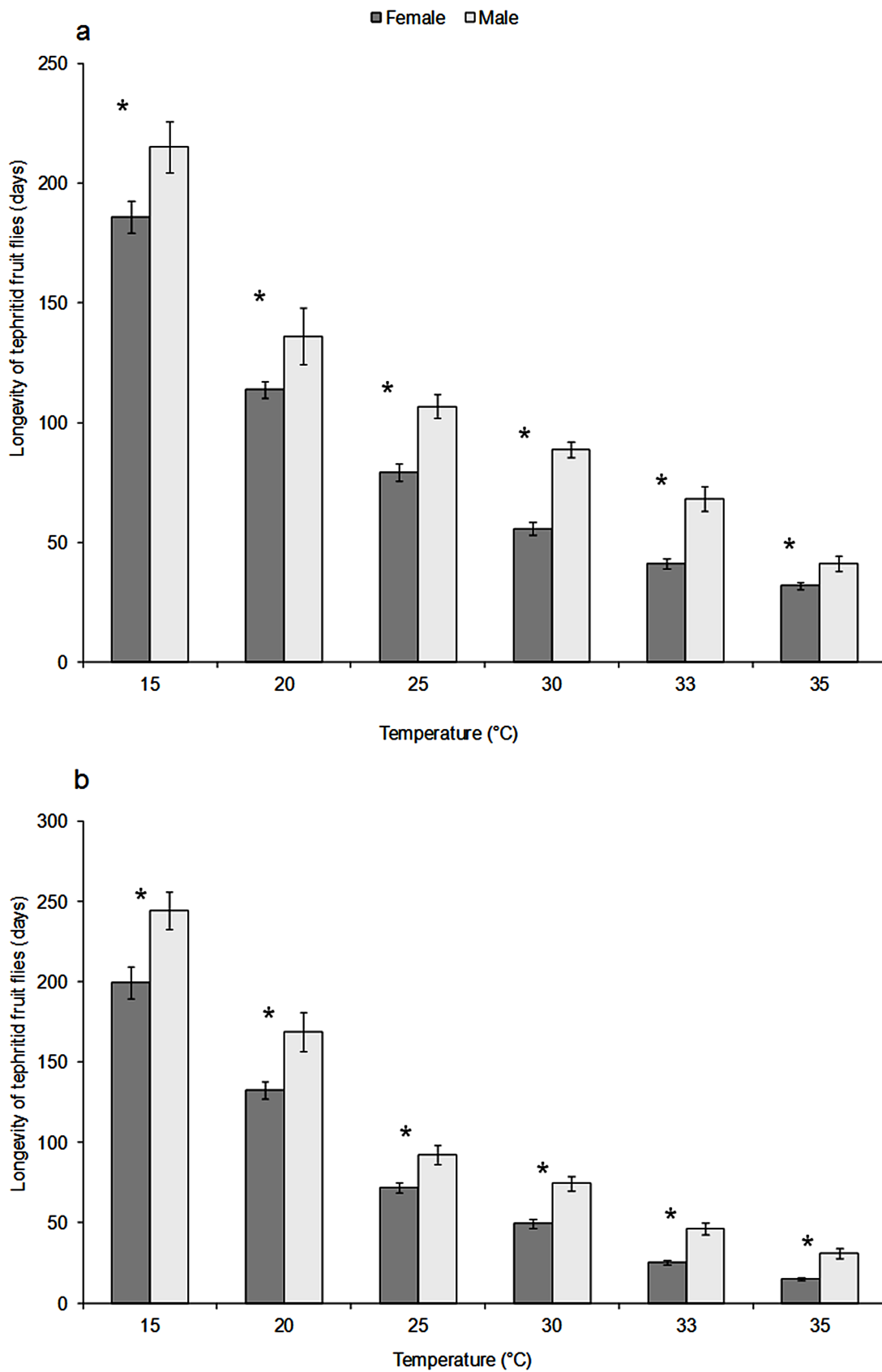


**Fig 3.** Mean longevity of females and males of *C. rosa* (3a) and *C. quilicci* (3b) at different temperature regimes. Asterisks above bars denote statistically significant differences comparing the sexes for each tested temperature category. Error bars represent the standard error generated from 15 replicates per condition.

<https://doi.org/10.1371/journal.pone.0189138.g003>

to  $36.96 \pm 1.06$  at  $35^{\circ}\text{C}$ . The shortest doubling time for *C. rosa* and *C. quilicci* were observed at  $30^{\circ}\text{C}$ . Fitting of a polynomial model to the estimated life table parameters predicted

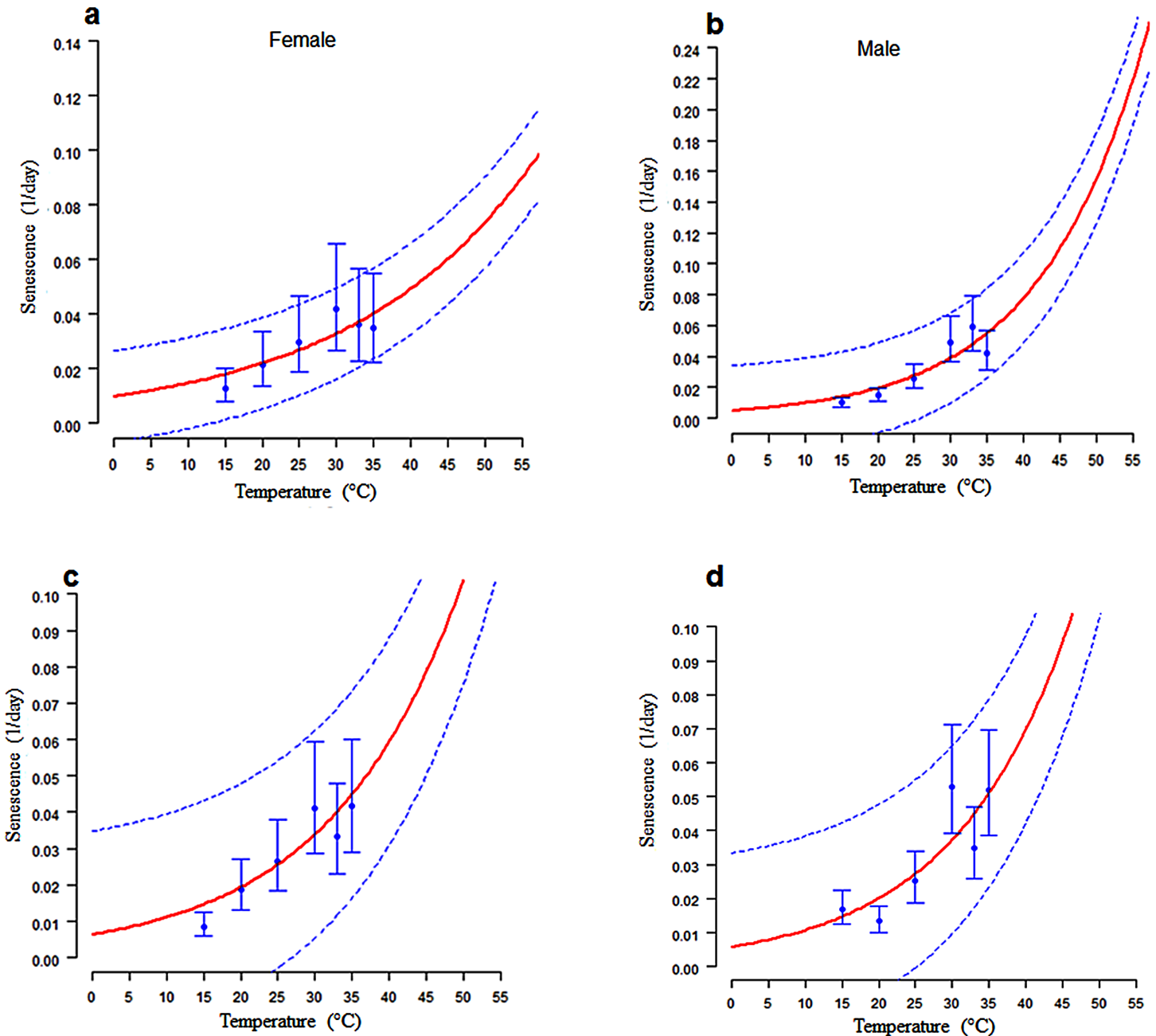


**Fig 4.** Temperature-dependent senescence rates (1/day) for adult *C. rosa* females (4a) and *C. rosa* males (4b); and for *C. quilicci* females (4c) and *C. quilicci* males (4d). Fitted curves: Exponential model for both sexes for each fruit fly species. The upper and lower 95% confidence intervals of the models are indicated. Bar represent standard deviation of the mean.

<https://doi.org/10.1371/journal.pone.0189138.g004>

**Table 5.** Estimated parameters (mean  $\pm$  SE) of the exponential function:  $r(T) = b1 \cdot \exp(b2 \cdot T)$ ; fitted to the mean senescence rates for adult life stages of *Ceratitis rosa* and *Ceratitis quilicci*.

	Life stage	Exponential function: $r(T) = b1 \cdot \exp(b2 \cdot T)$					
		b1	b2	$r^2$	F	df	P
<i>C. rosa</i>	Female	0.0098 (0.0041)	0.0403 (0.0137)	0.7470	11.8107	1,5	0.0264
	Male	0.0049 (0.0039)	0.0689 (0.0247)	0.7730	13.5979	1,5	0.0211
<i>C. quilicci</i>	Female	0.0061 (0.0029)	0.056 (0.0151)	0.8390	20.7951	1,5	0.0103
	Male	0.0058 (0.0042)	0.0624 (0.0234)	0.7280	10.7256	1,5	0.0306

Numbers in parentheses are standard errors of estimates

<https://doi.org/10.1371/journal.pone.0189138.t005>

temperatures between 25–30°C as the most favourable range for *C. rosa* (Fig 5A) and *C. quilicci* (Fig 5B) development, survival and reproduction.

### Phenological model validation

Model simulations with data collected under constant temperatures predicted good development duration and mortality in immature life stages when compared to the data collected under fluctuating temperatures for *C. rosa* and *C. quilicci* (Table 7 and Fig 6). Also, the simulated values of intrinsic rate of natural increase ( $r_m$ ), finite rate of population increase ( $\lambda$ ) and doubling time (Dt) generated at constant temperature regimes were closely similar to the observed values (Table 8), making the developed phenology models capable of properly simulating the demographic parameters.

### Spatial mapping: Changes in *C. rosa* and *C. quilicci* distribution and abundance

In Kenya, the model predicted that *C. rosa* is well established along the coastal region, and Lake Victoria (Fig 7A) with ERI values ranging between 0.87 and 1.0, while *C. quilicci* is highly restricted along the highlands of Western and Central Kenya, especially around Lake Victoria (Fig 7B). Although, *C. rosa* and *C. quilicci* have different ecological requirements, the model predicted areas of sympatry between the two species in some regions in Africa (ERI between 0.7 and 0.87). Under the present climatic conditions, the establishment risk index reflects well the current distribution *C. rosa* (Fig 8A) and *C. quilicci* (Fig 8B) in Eastern and Southern Sub-Saharan African countries, which includes Kenya, Tanzania, Uganda, Rwanda, Somalia,

**Table 6.** Life table parameters of *Ceratitis rosa* and *Ceratitis quilicci* estimated at different constant temperature regimes.

Parameters	Temperature (°C)											
	15		20		25		30		33		35	
	<i>C. rosa</i>	<i>C. quilicci</i>										
$r_m$	0.04±3.1x10 <sup>-3</sup> A	0.04±4.4x10 <sup>-4</sup> A	0.07±7.7x10 <sup>-4</sup> A	0.08±8.2x10 <sup>-4</sup> A	0.14±1.1x10 <sup>-3</sup> A	0.12±9.2x10 <sup>-4</sup> B	0.19±2.7x10 <sup>-3</sup> A	0.11±1.7x10 <sup>-3</sup> A	0.10±2.3x10 <sup>-3</sup> A	0.09±2.5x10 <sup>-3</sup> A	0.04±2.0x10 <sup>-3</sup> A	0.04±7.4x10 <sup>-3</sup> A
R <sub>o</sub>	28.25±2.17 <sup>a</sup> A	31.87±1.4 <sup>a</sup> A	79.88±4.32 <sup>a</sup> B	95.12±4.89 <sup>a</sup> A	121.50±4.15 <sup>a</sup> A	100.72±4.58 <sup>a</sup> A	189.17±5.49 <sup>a</sup> A	68.71±4.96 <sup>a</sup> B	25.29±2.15 <sup>a</sup> A	22.84±1.66 <sup>a</sup> A	4.61±0.62 <sup>a</sup> A	3.57±0.77 <sup>a</sup> A
GRR	84.20±5.56 <sup>a</sup> A	91.44±4.48 <sup>a</sup> A	218.30±9.32 <sup>a</sup> A	245.65±12.89 <sup>a</sup> A	300.40±14.95 <sup>a</sup> A	278.38±11.79 <sup>a</sup> B	397.87±21.64 <sup>a</sup> A	269.12±24.03 <sup>a</sup> B	198.65±18.24 <sup>a</sup> A	176.81±13.66 <sup>a</sup> A	112.29±19.48 <sup>a</sup> A	84.49±18.62 <sup>a</sup> B
T	84.57±0.58 <sup>a</sup> A	83.70±0.57 <sup>a</sup> A	59.23±0.15 <sup>a</sup> B	58.71±0.35 <sup>a</sup> B	44.24±0.25 <sup>a</sup> A	43.33±0.23 <sup>a</sup> A	35.87±0.23 <sup>a</sup> A	35.89±0.20 <sup>a</sup> A	35.47±0.28 <sup>a</sup> A	35.27±0.18 <sup>a</sup> A	37.50±0.96 <sup>a</sup> A	36.96±1.06 <sup>a</sup> A
$\lambda$	1.04±1.1x10 <sup>-3</sup> A	1.04±4.6x10 <sup>-4</sup> A	1.08±8.3x10 <sup>-4</sup> A	1.08±8.8x10 <sup>-4</sup> A	1.12±1.2x10 <sup>-3</sup> A	1.11±1.0x10 <sup>-3</sup> A	1.14±3.0x10 <sup>-3</sup> A	1.12±1.9x10 <sup>-3</sup> A	1.11±2.5x10 <sup>-3</sup> A	1.09±2.7x10 <sup>-3</sup> A	1.05±8.5x10 <sup>-3</sup> A	1.02±1.3x10 <sup>-3</sup> A
D <sub>t</sub>	17.80±0.48 <sup>a</sup> A	16.81±0.18 <sup>a</sup> A	9.40±0.09 <sup>a</sup> A	8.97±0.10 <sup>a</sup> A	6.53±0.07 <sup>cd</sup> A	6.68±0.06 <sup>a</sup> A	5.93±0.16 <sup>a</sup> A	6.06±0.08 <sup>a</sup> A	7.74±0.20 <sup>a</sup> A	7.95±0.25 <sup>a</sup> A	17.03±0.8 <sup>a</sup> A	26.41±6.67 <sup>a</sup> A

Means in the same column followed by the same upper case and in the same row followed by the same lower case letter are not significantly different [ANOVA and Student–Newman–Keul's (SNK) test, P < 0.05].  $r_m$ , intrinsic rate of natural increase; R<sub>o</sub>, net reproduction rate; GRR, gross reproduction rate; GT, mean generation time;  $\lambda$ , finite rate of increase; Dt, doubling time (days).

Adult female *C. rosa* and *C. quilicci* failed to reproduce at 37°C.

<https://doi.org/10.1371/journal.pone.0189138.t006>

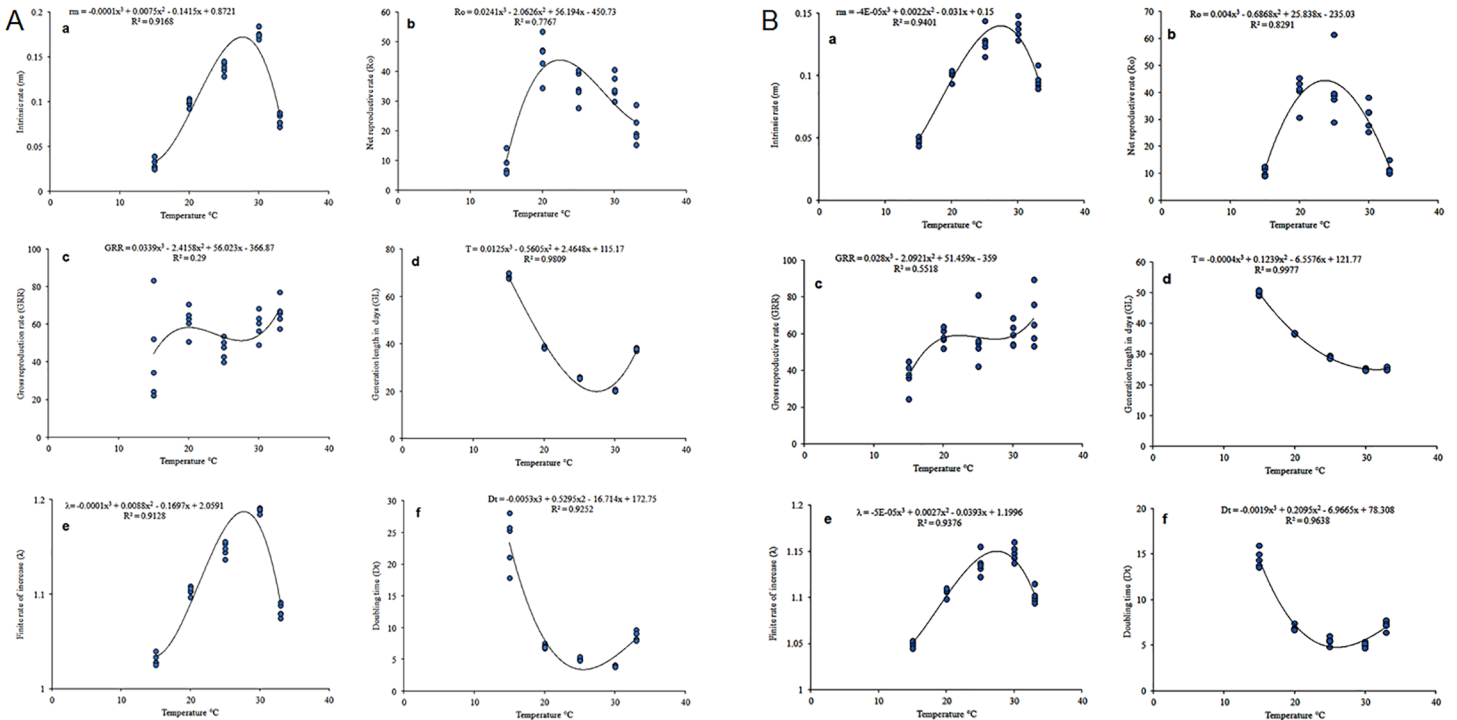


**Fig 5.** Life table parameters of *C. rosa* (5a) and *C. quilicci* (5b) estimated through model prediction over a range of six constant temperatures: Intrinsic rate of increase,  $r_m$ ; net reproduction rate,  $R_0$ ; gross reproductive rate, GRR; mean generation time, T; finite rate of increase,  $\lambda$ ; and doubling time,  $D_t$ .

<https://doi.org/10.1371/journal.pone.0189138.g005>

Zambia, Botswana, Eritrea, Ethiopia, Mozambique, Swaziland and Republic of South Africa. The model also indicates higher ERI values for *C. rosa* and *C. quilicci* in several countries in West and Central Africa (Guinea-Bissau, Guinea, Sierra Leone, Liberia, Côte d'Ivoire, Ghana, Togo, Benin, Nigeria, Cameroon, Central African Republic etc), although neither species have been recorded in these countries. The model predictions for the potential establishment of *C. rosa* (Fig 8A) and *C. quilicci* (Fig 8B) was validated by using known geo-referenced distribution data (Fig 8A and 8B).

**Table 7. Validation of the developed phenology model through comparison of observed and simulated developmental and mortality rates of *Ceratitis rosa* and *Ceratitis quilicci* life stages.**

		Eggs		Larvae		Pupa		Euclidian distance
		Developmental time (days)	Mortality (%)	Developmental time (days)	Mortality (%)	Developmental time (days)	Mortality (%)	
<i>C. rosa</i>	Simulated	2.325 ± 0.06	0.108 ± 0.06	9.105 ± 0.16	0.198 ± 0.06	11.873 ± 0.32	0.588 ± 0.18	Egg 6.40
	Observed	2.253 ± 0.15	0.151 ± 0.02	8.956 ± 0.10	0.139 ± 0.01	11.736 ± 0.12	0.662 ± 0.07	Larva 14.88
	P-value	0.0002	0.0045	0.0011	0.0005	0.0587	0.0657	Pupa 16.20
								Female 8.61
								Male 17.04
<i>C. quilicci</i>	Simulated	2.048 ± 0.11	0.102 ± 0.04	9.060 ± 0.12	0.165 ± 0.06	12.182 ± 0.16	0.594 ± 0.13	Egg 6.39
	Observed	2.098 ± 0.35	0.137 ± 0.21	9.100 ± 0.17	0.146 ± 0.09	12.019 ± 0.23	0.601 ± 0.19	Larva 10.99
	P-value	0.0404	0.0030	0.1552	0.1405	0.0006	0.8272	Pupa 8.89
								Female 9.18
								Male 11.12

Average ± SE: standard errors are calculated from the observed and simulated life table data

<https://doi.org/10.1371/journal.pone.0189138.t007>

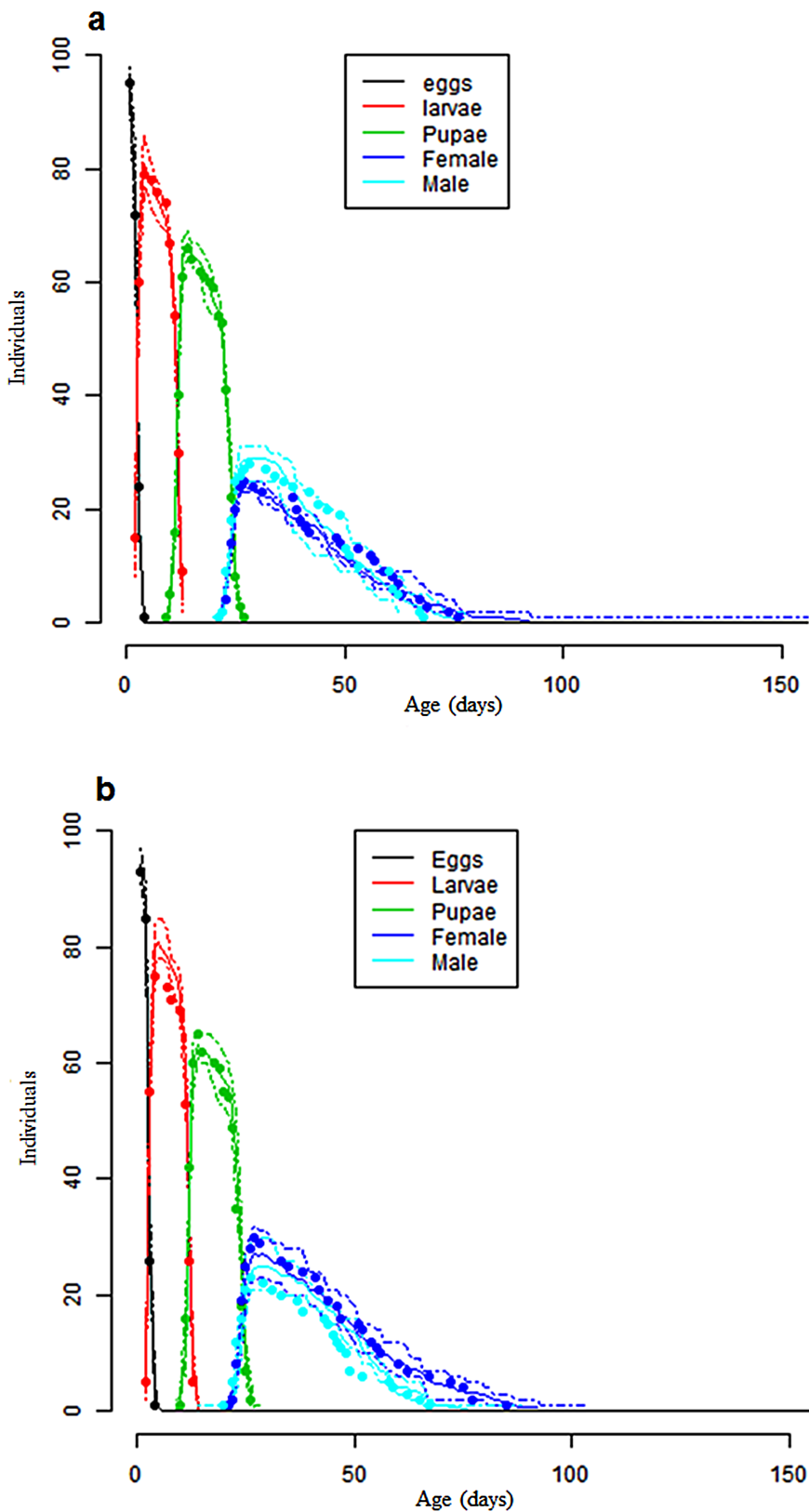


**Fig 6.** Model validation, observed and simulated life stage frequencies of *C. rosa* (6a) and *C. quilicci* (6b). Dots represent observed data points at fluctuating experiments, and the lines represent developmental

frequencies simulated at fluctuated temperatures based on thermal reaction norms for constant temperatures. Solid lines are averages of the 50 simulations while the broken lines indicate minimum and maximum value obtained from the 50 simulations.

<https://doi.org/10.1371/journal.pone.0189138.g006>

Additional countries where neither pest has been reported but were found to be potentially suitable areas for invasion included: Madagascar, Middle East, Oceania, South and Southeastern Asia, Australia, Mexico, all Caribbean islands, Southern and Central America ([Fig 9A](#) and [9B](#) for *C. rosa* and *C. quilicci*, respectively). The model also successfully predicted distinct broad potential ranges for *C. quilicci* in southern Europe and United States of America, which are not predicted to be suitable for *C. rosa*. The risk maps developed for the world with the climate data showed that areas with high-growth index (GI) ([Fig 10A](#) for *C. rosa* and [Fig 10B](#) for *C. quilicci*) also had high activity index (AI) ([Fig 11A](#) for *C. rosa* and [Fig 11B](#) for *C. quilicci*). However, it was found convenient to further evaluate the predictive ability of the model by estimating the potential number of generations of *C. rosa* ([Fig 10A](#)) and *C. quilicci* ([Fig 10B](#)), if they happen to invade and establish in different parts of around the world.

## Discussion

### Physiological effects of temperature

Our findings provide new evidence in support of the recent recognition that *C. rosa* comprises two distinct species, *C. rosa* and *C. quilicci* [61]. Whereas previous data was based on morphometrics, developmental physiology, cuticular hydrocarbons, pheromones and mating incompatibility studies, our study provides complementary evidence on distinct physiological differences between the two species in relation to temperature using climatic niche modelling. These findings agree with Mwatawala et al. [75] and Tanga et al. [3] who showed that the two species had different environmental requirements (lower developmental thresholds and development rates). The data confirms the hypothesis that *C. rosa* includes two separate entities with different ecological requirements [2]. This had been previously observed by Grout and Stoltz [2] and Duyck and Quilici [1], where the morphotype R1 (*C. rosa*) was dominant in lower altitude areas of South Africa whereas the morphotype R2 (*C. quilicci*) predominated in the high altitude area in Réunion [60]. The model also predicted areas of sympatry between the two species in the Mpumalanga and Kwa-Zulu Natal provinces of South Africa. The model was accurate and reliable in delineating climatic niche partitioning of *C. rosa* and *C. quilicci* and demonstrated that temperature remains one of the key factors that specifically determines the distribution range of both species. Our observation is further supported by the findings reported by Nyamukondwa et al [76], which shows that plasticity in acute thermal tolerance might also be an important mechanism facilitating survival of fruit fly species upon

**Table 8. Validation of the developed phenology model through comparison of observed and simulated population growth parameters of *Ceratitis rosa* and *Ceratitis quilicci*.**

Parameter	Population growth parameters					
	<i>C. rosa</i>			<i>C. quilicci</i>		
	Simulated	Observed	P-value	Simulated	Observed	P-value
r <sub>m</sub>	0.12 ± 0.02	0.108 ± 0.01	0.2350	0.095 ± 0.001	0.11 ± 0.01	0.0781
λ	1.09 ± 0.01	1.10 ± 0.01	0.1812	1.08 ± 0.02	1.10 ± 0.02	0.2125
Dt	10.74 ± 1.17	9.89 ± 0.45	0.3116	12.15 ± 2.18	12.03 ± 1.73	0.0975

Average ± SE: standard errors are calculated from the observed and simulated life table data

<https://doi.org/10.1371/journal.pone.0189138.t008>

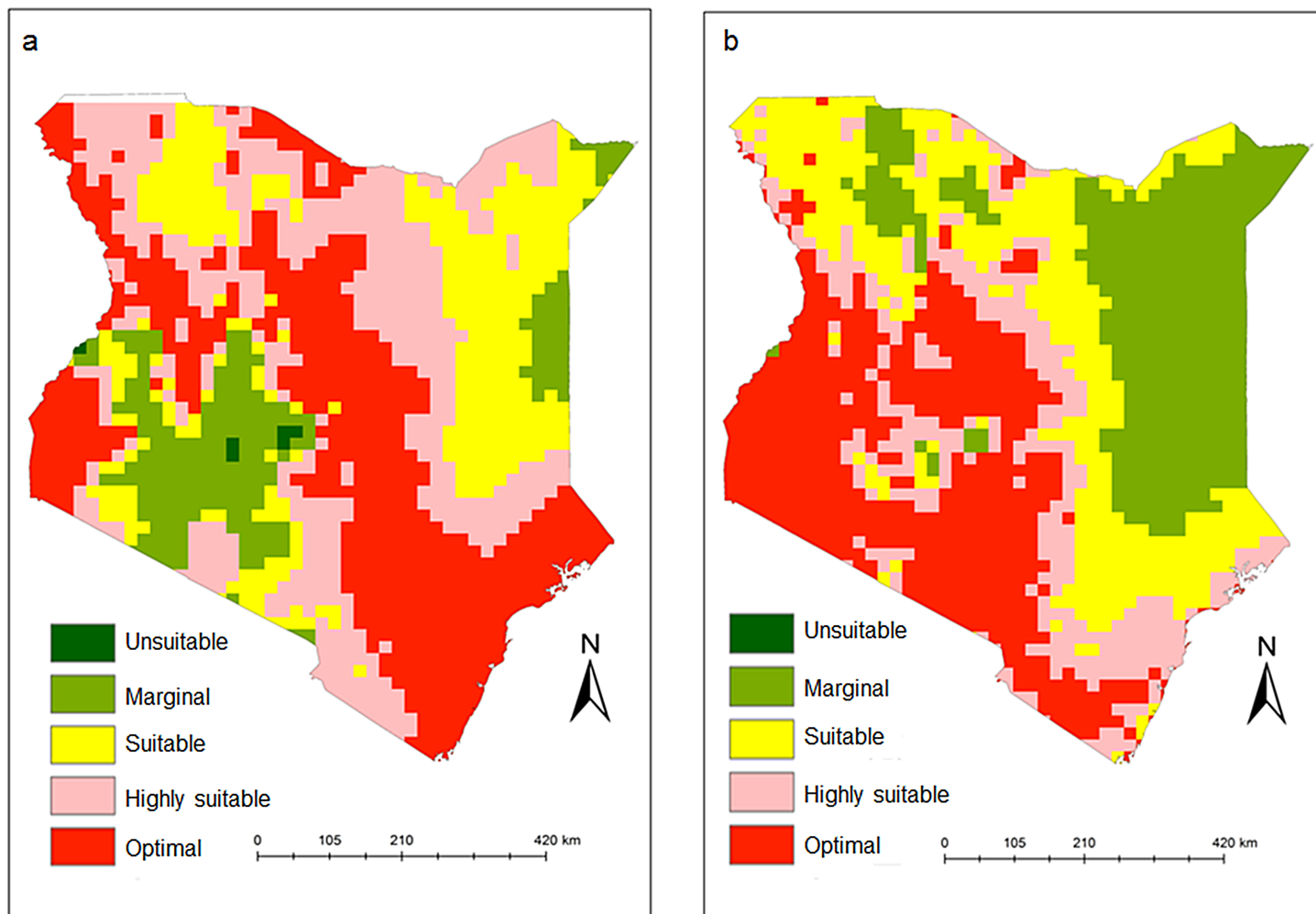


**Fig 7.** *Ceratitis rosa* (7a) and *C. quilicci* (7b) establishment risk index according to ILCYM model prediction in Kenya. Indices >0.6 is associated with potential permanent establishment. The ERI identifies the area in which the insect may survive and become established permanently.

<https://doi.org/10.1371/journal.pone.0189138.g007>

introduction to novel thermal environments due to variation in their physiological responses particularly in cooler and more thermally variable geographical regions, which may contribute to their ongoing invasion success relative to other fruit fly species.

Using the second-order polynomial function to describe the relationship between mortality and temperature, another key finding in the present study was the lower larval developmental threshold for *C. quilicci* Kenyan population ( $4.8^{\circ}\text{C}$ ), which was consistent with that reported by Duyck and Quilici [1] for the population ( $3.1^{\circ}\text{C}$ ) in Réunion. This suggests that *C. quilicci* is better adapted to lower temperatures in comparison with *C. capitata* ( $10.2^{\circ}\text{C}$ ) and the native *C. catoirii* ( $8.9^{\circ}\text{C}$ ), a native species in Réunion. Although, the lower larval developmental threshold of *C. rosa* ( $9.6^{\circ}\text{C}$ ) was found to be similar to that of *C. capitata* and *C. catoirii* [1,2], *C. rosa* has been reported to out-competed the latter species [18–21, 23–25]. While it is not clear to what extent these species co-exist in the wild throughout their native range, it is likely that each species dominates in particular regions of the climate space. Indeed, Duyck et al. [56] have shown that climatic factors and niche segregation between *C. capitata* and *C. rosa* influence the distribution of these species in Réunion. However, caution may be required in interpreting these findings as other factors besides temperature also play major role in the national

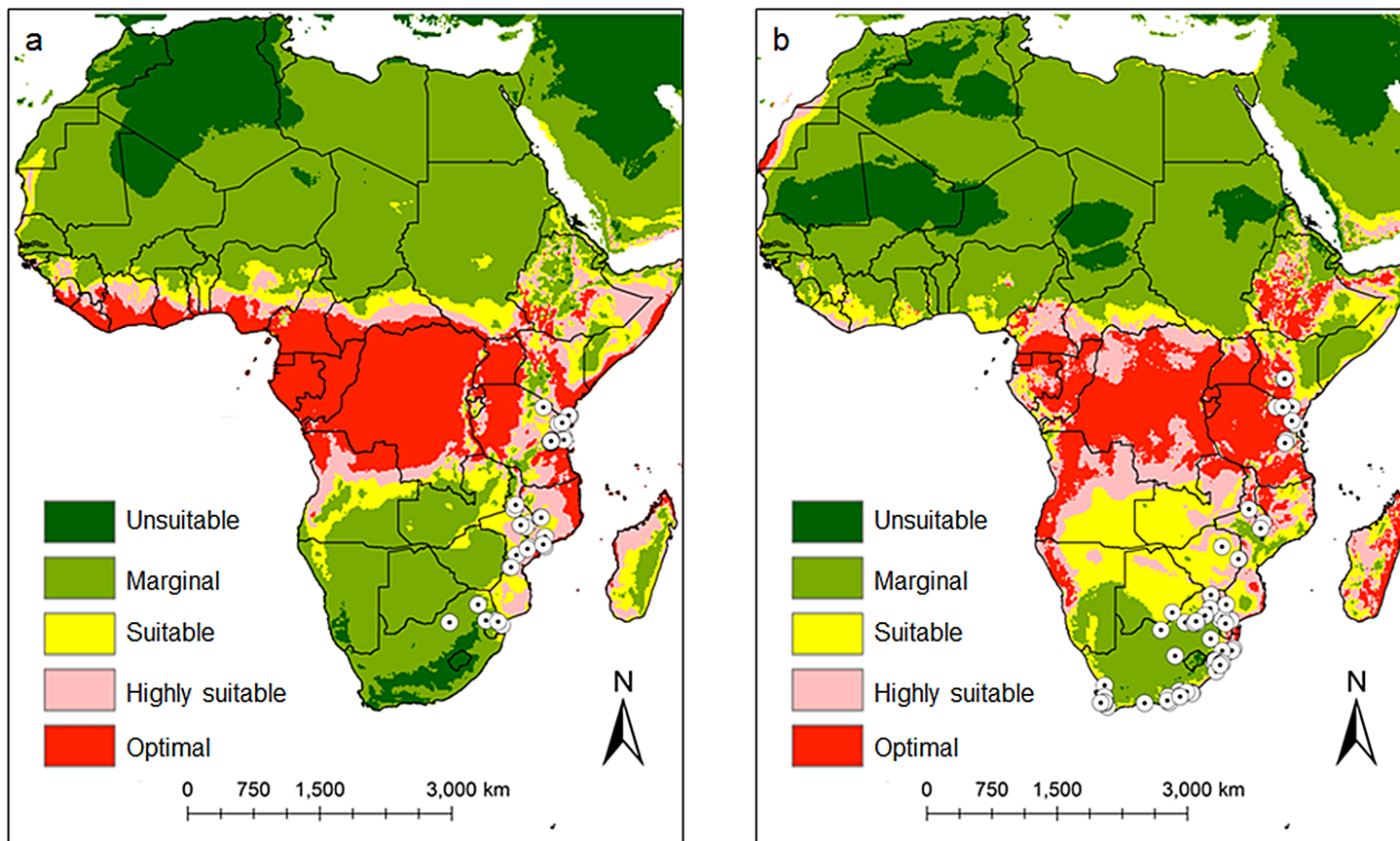


**Fig 8.** *Ceratitis rosa* (8a) and *C. quilicci* (8b) establishment risk index according to ILCYM model prediction in Africa, validated using known geo-referenced distribution data of each species. Indices > 0.6 are associated with potential permanent establishment. The ERI identifies the area in which the insect may survive and become established permanently.

<https://doi.org/10.1371/journal.pone.0189138.g008>

(local), regional and global invasion potential of insect species. For example, before invasion, major factors will include host preference and quality, relative humidity, tolerance of water stress, phenotypic plasticity, tourism and trade, climate change and land use, and after introduction dispersal can be influenced by high reproductive potential, rapid dispersal ability and broad host range [15,55–57, 68–70,76,78,88,89,90].

This study presents for the first time the preoviposition, oviposition and post-oviposition period of *C. rosa* and *C. quilicci* across different temperature regimes. However, the developmental duration of the immature life stages of the two species did not differ substantially from that reported by Duyck and Quilici [1] and, Grout and Stoltz [2]. The longest preoviposition period of *C. rosa* (58 d) and *C. quilicci* (43 d) was recorded at 15°C, while the shortest pre-oviposition period of *C. rosa* (10 d) and *C. quilicci* (11 d) was observed at 35°C. This deviates from the findings of Duyck and Quilici [1], who reported that *C. rosa* will not produce mature eggs at 15 and 35°C. Although, we observed ovarian maturation at 15 and 35°C, the survival rate of the adult flies was very low, which explains the limited number of eggs laid at both temperature extremes. In the present study, *C. rosa* achieved its highest intrinsic rate of increase (0.19) and net reproductive rate (189) at 30°C, which is comparable to that of *B. dorsalis* at the same temperature ( $r_m = 0.174$  and  $R_o = 196$ ) but higher than that of *C. capitata* ( $r_m = 0.137$  and  $R_o = 264.2$ ) [77, 78]. On the other hand, *C. quilicci* exhibited higher intrinsic rate of increase (0.14)

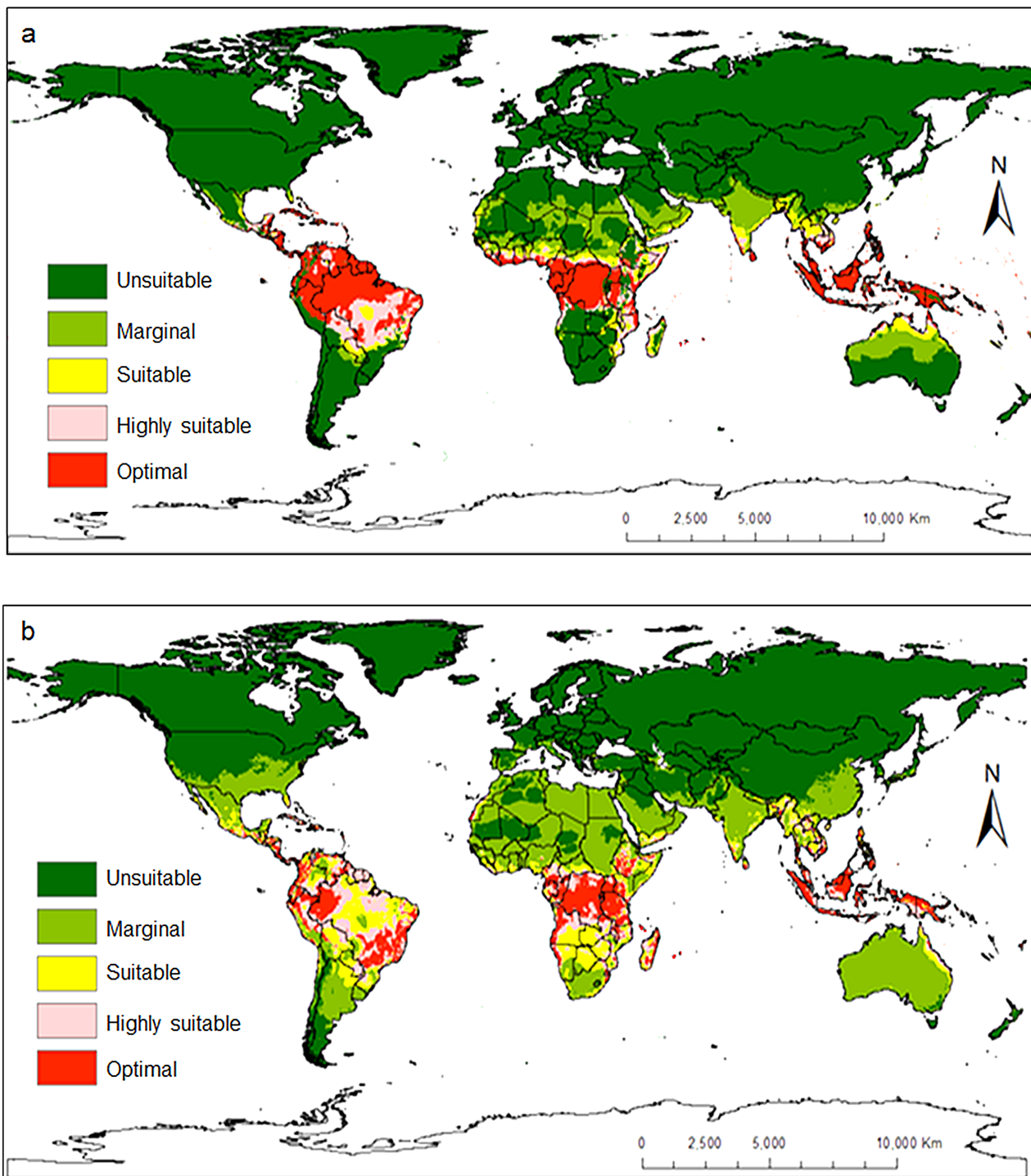


**Fig 9.** *Ceratitis rosa* (9a) and *C. quilicci* (9b) establishment risk index according to ILCYM model prediction in the world. Indices > 0.6 are associated with potential permanent establishment. The ERI identifies the area in which the insect may survive and become established permanently.

<https://doi.org/10.1371/journal.pone.0189138.g009>

and net reproductive rate (100.7) at 25°C than *C. cosyra* ( $r_m = 0.109$  and  $R_o = 96.6$ ) and *B. dorsalis* ( $r_m = 0.128$  and  $R_o = 30.5$ ) [77].

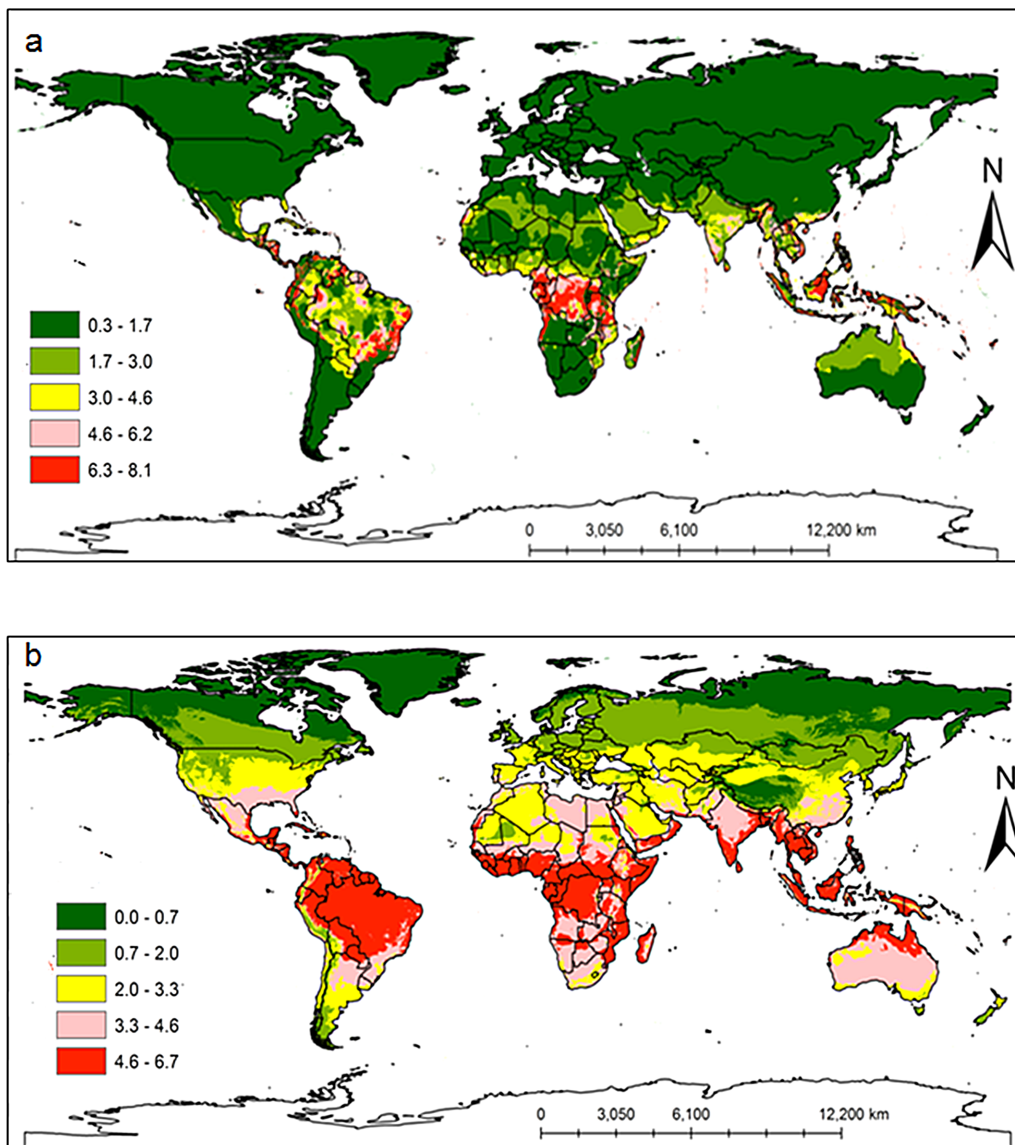


**Fig 10.** *Ceratitis rosa* (10a) and *C. quilicci* (10b) generation index (GI) according to ILCYM model predictions in the world. The GI estimates the mean number of generations that may be produced within a given year.

<https://doi.org/10.1371/journal.pone.0189138.g010>

The lifetime fecundity of *C. rosa* and *C. quilicci* reared within the temperature range of 20–30° was comparable to that of several fruit fly species including *C. capitata*, *B. dorsalis*, *B. zonata* and *Zeugodacus cucurbitaceae* etc, which are the most widespread fruit fly pests of soft fruits and vegetables globally. Our results also showed that temperature-dependent mortality rates of *C. rosa* and *C. quilicci* was significantly higher at temperature extremes (lower and upper thermal threshold). Based on high temperature variation between the *C. rosa* and *C. quilicci*, our results suggest that *C. rosa* is physiologically more adapted to higher temperatures than *C. quilicci*, which explains the observed distribution of both species in the Eastern and Southern regions of Africa, with *C. quilicci* being more restricted to the highlands [58, 59], while *C. rosa* is restricted in the lowlands [50]. The cold tolerant nature of *C. quilicci* particularly raises major concern outside of Africa and its invasive powers require close attention.

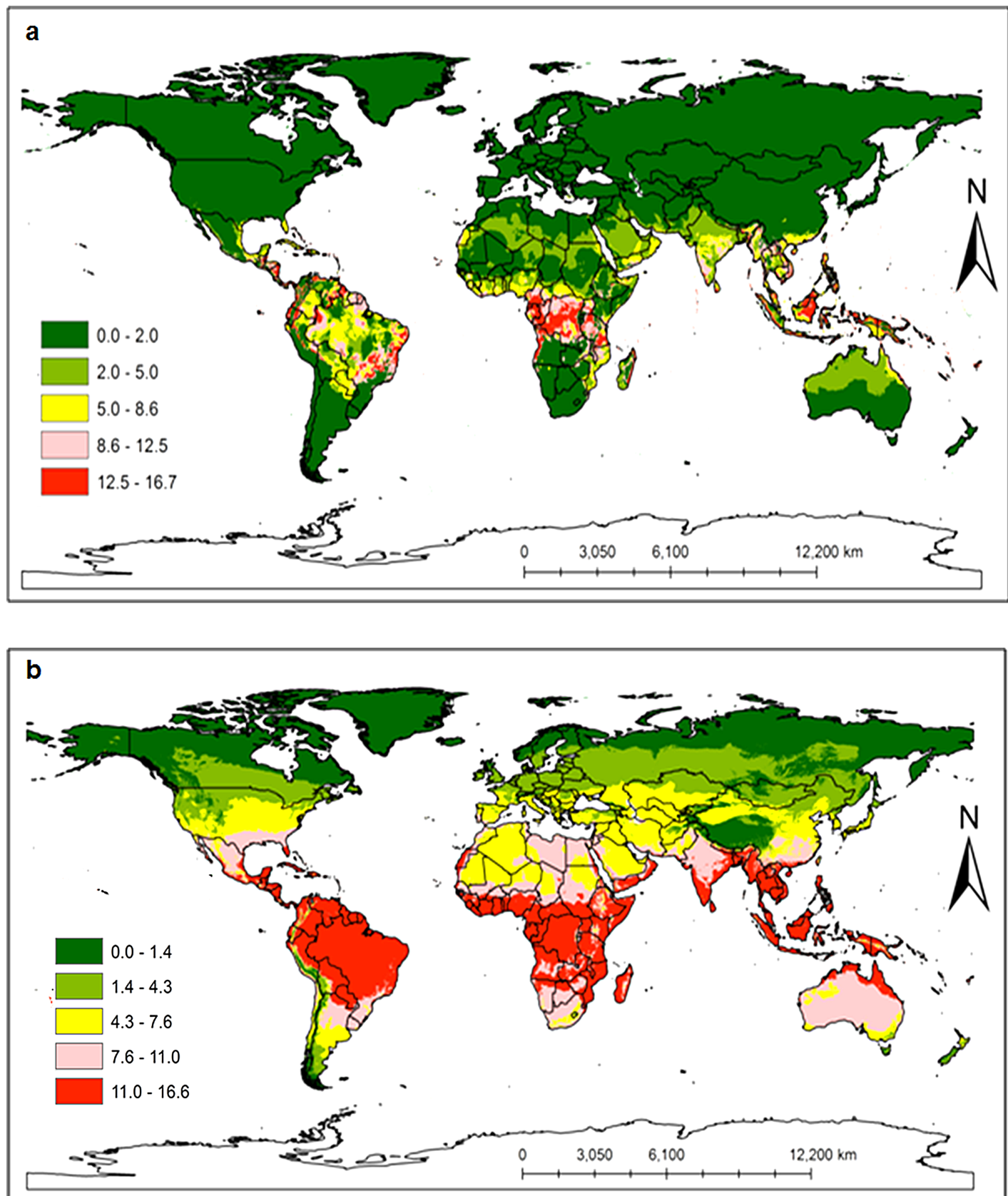


**Fig 11.** *Ceratitis rosa* (11a) and *C. quilicci* (11b) activity index (AI) according to ILCYM model predictions in the world. The AI takes the whole life history into consideration; an index value of 3 would illustrate a potential population increases by a factor of 1000 within one year.

<https://doi.org/10.1371/journal.pone.0189138.g011>

Overall, our observation agrees with the climatic variability hypothesis, which states that the thermal tolerance of an insect is directly proportional to the climate variability that the organism is exposed to [79].

### Prediction of the distribution of *C. rosa* and *C. quilicci*

Mapping the distribution of potentially invasive species is an iterative process. This is the first attempt at modelling the distribution of *C. rosa* and *C. quilicci* using temperature-dependent phenology models and projecting the risk of spread at national, regional and international level. Our models showed that *C. quilicci* will be more tolerant to a wider range of climatic conditions than *C. rosa*, occupying broader predicted regions than *C. rosa*. Results from the prediction showed that the current distribution and abundance of *C. rosa* and *C. quilicci* aligns with the occurrence data of both fruit fly species, which have been earlier reported from Eastern and Southern Africa [49,80,81]. Focusing on specific countries in the West and Central regions of Africa, we noted that these regions have a high risk of invasion and establishment of the pests and will threaten horticultural production in the region. Adequate phytosanitary management measures for fruits and vegetables proven to represent hosts of either species are recommended to curb the spread of both fruit fly species.

Risk maps also showed that the following countries and regions may be suitable for establishment of *C. rosa* and *C. quilicci*—Madagascar, the Middle East, Oceania, South and Southeast Asia, a large section of Australia, Mexico, all Caribbean islands, and Southern and Central America. The model also showed that *C. quilicci* has a broader distinct potential range of suitability in the southern regions of Europe and the United States of America (USA), but this was not the case for *C. rosa*. The area highly suitable for *C. rosa* in the USA was limited only to southern Florida. These findings are consistent with earlier studies by De Meyer et al. [10], who used correlative ecological niche modeling techniques based on genetic algorithm for rule-set prediction (GARP) and principal components analysis (PCA) to predict the global distribution of *C. rosa*. However, we believe that the incorporation of other known climatic drivers such as host plant diversity, natural enemy dynamics, relative humidity and rainfall that influence tephritid fruit fly species dynamics would enhance the validity of the predictions in the present studies [1,47,41,82,83, 88].

The global risk maps for both species showed that the areas with high-growth index (GI) also had high activity index (AI). The generation indices simulated for *C. quilicci* revealed that it was capable of completing 5–7 generations in a year, whereas *C. rosa* had 7–8 generations per year. These observations closely mirror the generation times that have been reported for several other tephritid fruit fly species [84–86].

Although the host range of *C. quilicci* has not been fully documented after having been proposed as a new species, we speculate that this might not be too different from those of *C. rosa* that also parallel those of *C. capitata* [34,87,80,1,10,3]. Together, these species represent a major threat to the horticulture industry in Africa and beyond, due to their capacity to become established and invade regions of the world outside their native range [10,81] based on the data presented here. Also, due to the significant differences in developmental rates of immatures, important population parameters such as the intrinsic rate of increase, survival and reproductive patterns of both *C. rosa* and *C. quilicci*, coupled with the lack of competitors and efficient natural enemies, and further compounded with the poor quarantine infrastructure in areas already invaded [18–21, 23–25], their invasion dynamics might be affected [88,89] such

that the species turned to spread widely to new locations with far reaching social and economic consequences. Thus, this offers plausible justification to continue to assess their potential for establishment and spread.

The present study highlights the importance of temperature on the developmental rate, mortality, oviposition, fecundity and longevity of *C. rosa* and *C. quilicci*. Prediction of tephritid fruit fly pest phenology is an important component of developing a management strategy for potentially invasive pests. Overall, the proportion of the regions predicted to be highly suitable was found to be broader for *C. quilicci* than *C. rosa*, suggesting that *C. quilicci* may be tolerant to a wider range of climatic conditions than *C. rosa*. This raises major concerns for the global horticulture industry as both species tend to have high invasive powers and have the potential to out-compete other tephritid fruit flies [10]. These concerns are further compounded by low phytosanitary skills in the region. However, our findings provide important information to enhance monitoring and surveillance, and designing of local, regional and national-level phytosanitary and integrated pest management to curb the spread and potential establishment of both pest species across Africa and beyond. There is also a pressing need to carefully establish the host range of each species, and the susceptibility of fruits and vegetables at different stages of development when grown commercially for export.

## Acknowledgments

Early drafts of the manuscript benefited from the useful comments of M. De Meyer (Royal Museum for Central Africa) and his substantial contribution is gratefully acknowledged. The authors also wish to thank Dr. Daisy Salifu and two anonymous referees for their valuable editorial comments on the first version of the text. The authors are also grateful to Peterson Nderitu for providing technical support during data collection.

This research was financially supported by the International Atomic Energy Agency (IAEA), through the CRP on “Resolution of Cryptic Species Complexes of Tephritid Pests to Overcome Constraints to SIT Application and International Trade, and EU-IBCARP Fruit Fly Project (DCI-FOOD/2014/346-739) through the International Centre of Insect Physiology and Ecology (icipe). We also gratefully acknowledge the icipe core funding provided by UK Aid from the Government of the United Kingdom; Swedish International Development Cooperation Agency (Sida); the Swiss Agency for Development and Cooperation (SDC); Federal Ministry for Economic Cooperation and Development (BMZ), Germany, and the Kenyan Government. The views expressed herein do not necessarily reflect the official opinion of the donors.

## Author Contributions

**Conceptualization:** Chrysantus Mbi Tanga, Fathiya Mbarak Khamis, Henri E. Z. Tonnang, Ivan Rwomushana, Samira A. Mohamed, Sunday Ekesi.

**Data curation:** Chrysantus Mbi Tanga, Sunday Ekesi.

**Formal analysis:** Chrysantus Mbi Tanga, Fathiya Mbarak Khamis, Henri E. Z. Tonnang, Samira A. Mohamed, Sunday Ekesi.

**Funding acquisition:** Samira A. Mohamed, Sunday Ekesi.

**Investigation:** Chrysantus Mbi Tanga, Fathiya Mbarak Khamis, Henri E. Z. Tonnang, Samira A. Mohamed, Sunday Ekesi.

**Methodology:** Chrysantus Mbi Tanga, Fathiya Mbarak Khamis, Henri E. Z. Tonnang, Ivan Rwomushana, Samira A. Mohamed.

**Project administration:** Chrysantus Mbi Tanga, Henri E. Z. Tonnang, Samira A. Mohamed, Sunday Ekesi.

**Resources:** Chrysantus Mbi Tanga, Samira A. Mohamed, Sunday Ekesi.

**Software:** Chrysantus Mbi Tanga, Henri E. Z. Tonnang, Sunday Ekesi.

**Supervision:** Henri E. Z. Tonnang, Samira A. Mohamed, Sunday Ekesi.

**Validation:** Chrysantus Mbi Tanga, Fathiya Mbarak Khamis, Henri E. Z. Tonnang, Ivan Rwmushana, Gladys Mosomtai, Samira A. Mohamed, Sunday Ekesi.

**Visualization:** Chrysantus Mbi Tanga, Fathiya Mbarak Khamis, Henri E. Z. Tonnang, Ivan Rwmushana, Gladys Mosomtai, Samira A. Mohamed, Sunday Ekesi.

**Writing – original draft:** Chrysantus Mbi Tanga, Fathiya Mbarak Khamis, Henri E. Z. Tonnang, Ivan Rwmushana, Gladys Mosomtai, Samira A. Mohamed, Sunday Ekesi.

**Writing – review & editing:** Chrysantus Mbi Tanga, Fathiya Mbarak Khamis, Henri E. Z. Tonnang, Ivan Rwmushana, Gladys Mosomtai, Samira A. Mohamed, Sunday Ekesi.

## References

1. Duyck PF, Quilici S (2002) Survival and development of different life stages of three *Ceratitis* spp. (Diptera: Tephritidae) reared at five constant temperatures. Bull Entomol Res 92: 461–469. PMID: [17598297](https://doi.org/10.1080/0007414021017598297)
2. Grout TG, Stoltz KC (2007) Developmental rates at constant temperature of three economically important *Ceratitis* spp. (Diptera: Tephritidae) from Southern Africa. Environ Entomol 36: 1310–1317. PMID: [18284758](https://doi.org/10.1603/0046-2865(2007)36[1310:DROSAT]2.0.CO;2)
3. Tanga MC, Manrakhan A, Daneel J-H, Mohamed SA, Khamis F, Ekesi S (2015) Comparative analysis of development and survival of two Natal fruit fly *Ceratitis rosa* Karsch (Diptera, Tephritidae) populations from Kenya and South Africa. ZooKeys 540: 467–87.
4. Fletcher B.S. (1989) Temperature–development rate relationships of the immature stages and adults of tephritid fruit flies. In: Robinson AS, Hooper G (Eds) Fruit flies their biology, natural enemies and control, Vol. 3A. Elsevier, Amsterdam.
5. Yang P, Carey JR, Dowell RV (1994a) Host specific demographic studies of wild *Bactrocera tau* (Walker) (Diptera: Tephritidae). Pan-Pac Entomol 70(3): 253–258.
6. Yang P, Carey JR, Dowell RV (1994b) Temperature influences on the development and demography of *Bactrocera dorsalis* (Diptera: Tephritidae) in China. Environ Entomol 23: 971–974.
7. Xiaofei L, Hui Y (2009) Effect of temperature on development and survival of *Bactrocera correcta* (Diptera: Tephritidae). Sci. Res. Essays 4 (5): 467–472.
8. Marshall WJ, Wang XG, Nadel H, Opp SB, Lynn-Patterson K, Stewart-Leslie J, Daane KM (2011) High temperature affects olive fruit fly populations in California's Central Valley. Calif Agric 65(1): 29–33.
9. Danjuma S, Thaochan N, Permkan S, Satasook C (2014) Effect of temperature on the development and survival of immature stages of the carambola fruit fly, *Bactrocera carambolae*, and the Asian papaya fruit fly, *Bactrocera papayae*, reared on guava diet. J Insect Sci 14: 126. <https://doi.org/10.1093/jis/14.1.126> PMID: [25368070](https://doi.org/10.1093/jis/14.1.126)
10. De Meyer M, Robertson MP, Peterson AT, Mansell MW (2008) Ecological niches and potential geographical distributions of Mediterranean fruit fly (*Ceratitis capitata*) and Natal fruit fly (*Ceratitis rosa*). J Biogeogr 35: 270–281.
11. Ekesi S, Mohamed SA (2010) *Bactrocera invadens*: State of the art and future research. TEAM Newsletter No. 8 (July 2010) TEAM Newsletter No. 8.
12. Pearson RG, Dawson TP (2003) Predicting the impacts of climate change on the distribution of species: are bioclimate envelope models useful? Global Ecol Biogeogr 12: 361–371.
13. Estay SA, Lima M, Labra FA (2009) Predicting insect pest status under climate change scenarios: combining experimental data and population dynamics modeling. J Appl Entomol 133: 491–499.
14. Baker CRB (1991) The validation and use of a life-cycle simulation model for risk assessment of insect pests. Bulletin OEPP 21: 615–622.

15. Kroschel J, Sporleder J, Tonnang HEZ, Juarez H, Carhuapoma JC, Simon R (2013) Predicting climate-change-caused changes in global temperature on potato tuber moth *Phthorimaea operculella* (Zeller) distribution and abundance using phenology modeling and GIS mapping. *Agric For Meteorol* 170: 228–241.
16. Trnka M, Muška F, Semerádová D, Dubrovský M, Kocmánková E, Žalud Z (2007) European corn borer life stage model: regional estimates of pest development and spatial distribution under present and future climate. *Ecol Model* 207(2): 61–84.
17. Beaumont JL, Hughes L, Poulsen M (2005) Predicting species distributions: use of climate parameters in BIOCLIM and its impact on predictions of species current and future distribution. *Ecol Model* 186: 250–269.
18. Sutherst RW, Maywald G (2005) A climate model of the red imported fire ant, *Solenopsis invicta* Buren (Hymenoptera: Formicidae): implications for invasion of new regions, particularly Oceania. *Environ Entomol* 34(2): 317–335.
19. Peacock L, Worner S (2006) Using analogous climates and global insect pest distribution data to identify potential sources of new invasive insect pests in New Zealand. *New Zeal J Zool* 33: 141–145.
20. Legaspi JC, Legaspi BC Jr (2007) Bioclimatic model of the spined soldier bug (Heteroptera, Pentatomidae) using CLIMEX: testing model predictions at two spatial scales. *J Entomol Sci* 42: 533–547.
21. Curry GL, Feldman RM, Smith KC (1978) Stochastic model for a temperature-dependent population. *Theor Popul Biol* 13: 197–213. PMID: 694782
22. Sporleder M, Kroschel J, Quispe MRG, Lagunaoui A (2004) A temperature-based simulation model for the potato tuberworm, *Phthorimaea operculella* Zeller (Lepidoptera: Gelechiidae). *Environ Entomol* 33 (3): 477–486.
23. Nietschke BS, Borchert DM, Magarey RD, Calvin DD, Jones E (2007) A developmental database to support insect phenology models. *Crop Prot* 26: 1444–1448.
24. Sporleder M, Simon R, Juarez H, Kroschel J (2008) Regional and seasonal forecasting of the potato tuber moth using a temperature-driven phenology model linked with geographic information systems. pp. 15–30. in Kroschel J. & Lacey L. (Eds) Integrated Pest management for the Potato Tuber Moth, *Phthorimaea operculella* Zeller—a Potato Pest of Global Importance. Tropical Agriculture 20, Advances in Crop Research 10. Weikersheim, Germany, Margraf Publishers.
25. Roitsch WJ, Mayse MA, Clausen K (1990) Temperature-dependent development under constant and fluctuating temperatures: comparison of linear versus nonlinear methods for modeling development of western rapeleaf skeletonizer (Lepidoptera: Zygaenidae). *Environ Entomol* 19(6): 1689–1697.
26. Stinner RE, Gutierrez AP, Butler GD Jr (1974) An algorithm for temperature-dependent growth rate simulation. *Can Entomol* 106: 519–524.
27. Hilbert DW, Logan JA (1983) Empirical model of nymphal development for the migratory grasshopper, *Melanoplus sanguinipes* (Orthoptera: Acrididae). *Environ Entomol* 12: 1–5.
28. Logan JA, Wollkind DJ, Hoyt SC, Tanigoshi LK (1976) An analytic model for description of temperature dependent rate phenomena in arthropods. *Environ Entomol* 5(6): 1133–1140.
29. Sharpe PJ, DeMichele DW (1977) Reaction kinetics of poikilotherm development. *J Theor Biol* 64(4): 649–670. PMID: 846210
30. Briere JF, Pracros P, Le Roux AY, Pierre JS (1999) A novel rate model of temperature-dependent development for arthropods. *Environ Entomol* 28(1): 22–29.
31. Sharpe PJ, Schoolfield RM, Butler GD Jr (1981) Distribution model of *Heliothis zea* (Lepidoptera: Noctuidae) development times. *Can Entomol* 113: 845–855.
32. Wagner TL, Wu HI, Sharpe PJ, Schoolfield RM, Coulson RN (1984) Modeling insect development rates: a literature review and application of a biophysical model. *Ann Entomol Soc Am* 77(2): 208–225.
33. Wagner TL, Olson RL, Willers JL (1991) Modeling arthropod development time. *J Agric Entomol* 8: 251–270.
34. White IM, Elson-Harris MM (1994) Fruit flies of economic significance: their identification and bionomics. 2<sup>nd</sup> ed. International Institute of Entomology, London.
35. Delgado CL, Siamwalla A (1997) Rural economy and farm income diversification in developing countries. MSSD Discussion paper no. 20, International Food Policy Research Institute, Washington, D.C.
36. Weinberger K, Lumpkin TA (2007) Diversification into horticulture and poverty: A research agenda. *World Dev* 35: 1464–1480.
37. Allwood AJ, Drew RAI (1997) Management of Fruit Flies in the Pacific, ACIAR Proceedings No. 76, A regional Symposium, Nadi, Fiji.
38. Barnes B (2004) Proceedings of the 6th International Symposium on Fruit Flies of Economic Importance. Ultra Litho (Pty), Johannesburg 510 pp.

39. Ekesi S, Billah MK (2007) A field guide to the management of economically important tephritid fruit flies in Africa. ICIPE Science Press, Nairobi, Kenya.
40. Lux SA, Copeland RS, White IM, Manrakan A, Billah MK (2003) A new invasive fruit fly species from the *Bactrocera dorsalis* (Hendel) group detected in East Africa. Insect Sci Appl 23: 355–361.
41. Ekesi S, Nderitu PW, Rwomushana I (2006) Field infestation, life history and demographic parameters of *Bactrocera invadens* Drew, Tsuruta & White, a new invasive fruit fly species in Africa. Bull Entomol Res 96: 379–386. PMID: [16923206](#)
42. Mwatawala MW, De Meyer M, Makundi RH, Maerere AP (2006a) Seasonality and host utilization of the invasive fruit fly, *Bactrocera invadens* (Diptera: Tephritidae) in Central Tanzania. J Appl Entomol 130 (9–10): 530–537.
43. Gnanssou D, Hanna R, Azandémè G, Goergen G, Tindo M, Agbaka A (2008) Inventaire et importance des dégâts des mouches des fruits sur quelques espèces de cucurbitacées au Bénin, pp 140–145. In Adjanohoun, A., et Igué, K (eds.). Actes de l'Atelier Scientifique National 6, Décembre 2006, Abomey-Calavi. Tome 1. ISBN 978-99919-6850-6; ISSN 1659-6161; Dépôt légal n° 3838 du 13/08/2008 3ème Trimestre. Bibliothèque Nationale du Bénin, 440pp.
44. Vayssières JF, Sanogo F, Noussorou M (2008b) The mango tree in central and northern Benin: Cultivar inventory, yield assessment, infested stages and loss due to fruit flies (Diptera: Tephritidae). Fruits 63: 335–348.
45. Burrack HJ, Fornell AM, Connell JH, O'connell NV, Phillips PA, Vossen PM, Zalom FG (2009) Intraspecific Larval Competition in the Olive Fruit Fly (Diptera: Tephritidae). Environ Entomol 38(5): 1400–1410. PMID: [19825295](#)
46. Vayssières JF, Sinzogan A, Adandonon A (2009a) Range of cultivated and wild hosts plants of the main mango fruit fly species in Benin. IITA-CIRAD Leaflet No 8.
47. Ekesi S, Mohamed SA (2011) Mass Rearing and Quality Control Parameters for Tephritid Fruit Flies of Economic Importance in Africa, Wide Spectra of Quality Control, Dr. Isin Akyar (Ed.), ISBN: 978-953-307-683-6, InTech, Available from: <http://www.intechopen.com/books/wide-spectra-of-qualitycontrol/>.
48. Ekesi S, Mohamed SA (2010) *Bactrocera invadens*: State of the art and future research. TEAM Newsletter No. 8 (July 2010) TEAM Newsletter No. 8.
49. White IM, Elson-Harris MM (1992) Fruit flies of economic importance: their identification and bionomics. CAB International, Wallingford, Oxon, and the Australian Center for Agricultural Research, Canberra, Australia 601 pp.
50. De Meyer M (2001a) On the identity of the Natal fruit fly *Ceratitis rosa* Karsch (Diptera, Tephritidae). Bulletin de l'Institut royal des Sciences Naturelles de Belgique, Entomologie 71: 55–62.
51. Orian AJE, Moutia LA (1960) Fruit flies (Tephritidae) of economic importance in Mauritius. Revue Agricole et Sucrière de l'Ile Maurice 39: 142–150.
52. Hancock DL (1989) World Crop Pests. Fruit flies, their biology, natural enemies and control, 3(A) Pest status. Southern Africa ( Elsevier, Amsterdam) pp 51–57.
53. Normand F, Quilici S, Simiand C (2000) Seasonal occurrence of fruit flies in strawberry guava (*Psidium cattleianum* Sabine) in Reunion Island: host phenology and fruit infestation. Fruits 55: 271–281.
54. White IM, De Meyer M, Stonehouse J (2001) A review of the native and introduced fruit flies (Diptera, Tephritidae) in the Indian Ocean Islands of Mauritius, Réunion, Rodrigues and Seychelles. Proceedings of the Indian Ocean Commission Regional Fruit Fly Symposium 15–21.
55. Duyck PF, David P, Quilici S (2004) A review of relationships between interspecific competition and invasions in fruit flies (Diptera: Tephritidae). Ecol Entomol 29: 511–520.
56. Duyck PF, David P, Quilici S (2006) Climatic niche partitioning following successive invasions by fruit flies in La Réunion. J Anim Ecol 75: 518–526. <https://doi.org/10.1111/j.1365-2656.2006.01072.x> PMID: [16638004](#)
57. Duyck PF, David P, Quilici S (2007) Can more K-selected species be better invaders? A case study of fruit flies in La Réunion. Divers Distrib 13 (5): 535–543.
58. Copeland RS, Wharton RA (2006) Year-round production of pest Ceratitis species (Diptera: Tephritidae) in fruit of the invasive species *Solanum mauritianum* in Kenya. Ann Entomol Soc Am 99: 3530–3535.
59. Barr NB, Copeland RS, De Meyer M, Masiga D, Kibogo HG, Billah M, Osir E, Wharton RA, McPheron BA (2006) Molecular diagnostics of economically important Ceratitis fruit fly species (Diptera: Tephritidae) in Africa using PCR and RFLP analyses. Bull Entomol Res 96: 505–521. PMID: [17092362](#)
60. Virgilio M, Delatte H, Quilici S, Backeljau T, De Meyer M (2013) Cryptic diversity and gene flow among three African agricultural pests: *Ceratitis rosa*, *Ceratitis fasciventris* and *Ceratitis anonaiae* (Diptera, Tephritidae). Mol Ecol 22: 2526–2539. <https://doi.org/10.1111/mec.12278> PMID: [23506441](#)

61. De Meyer M, Delatte H, Ekesi S, Jordaens K, Kalinova B, Manrakhan A, Mwatawala M, Steck G, Cann JV, Vancikova L, Brizova R, Virgilio M (2015) An integrative approach to unravel the *Ceratitis* FAR (Diptera, Tephritidae) cryptic species complex: a review. *ZooKeys* 540: 405–427.
62. Steck GJ, Ekesi S (2015) Description of third instar larvae of *Ceratitis fasciventris*, *C. anonae*, *C. rosa* (FAR complex) and *C. capitata* (Diptera, Tephritidae). *Zookeys* 540: 443–466.
63. Vaníčková L, Břízová R, Pompeiano A, Ekesi S, De Meyer M (2015) Cuticular hydrocarbons corroborate the distinction between lowland and highland Natal fruit fly (Tephritidae, *Ceratitis rosa*) populations. In: De Meyer M, Clarke AR, Vera MT, Hendrichs J. (Eds) Resolution of Cryptic Species Complexes of Tephritis Pests to Enhance SIT Application and Facilitate International Trade. *ZooKeys* 540: 507–524.
64. De Meyer M, Mwatawala M, Copeland RS, Virgilio M (2016) Description of new *Ceratitis* species (Diptera: Tephritidae) from Africa, or how morphological and DNA data are complementary in discovering unknown species and matching sexes. *Eur J Taxon* 233: 1–23. <http://dx.doi.org/10.5852/ejt.2016.233>
65. Honé A, Kocourek F (1990) Temperature and development time in insects: a general relationship between thermal constants. *Zool Jahrb Syst* 117: 401–439.
66. Rwmushana I, Ekesi S, Ogol CKPO, Gordon I (2008) Effect of temperature on development and survival of immature stages of *Bactrocera invadens* (Diptera: Tephritidae). *J Appl Entomol* 132: 832–839.
67. Ekesi S, Nderitu PW, Chang CL (2007) Adaptation to and small scale rearing of invasive fruit fly *Bactrocera invadens* (Diptera: Tephritidae) on artificial diet. *Ann Entomol Soc Am* 100: 562–567.
68. Sporleder M, Tonnang HEZ, Carhuapoma P, Gonzales JC, Juarez H, Kroschel J (2013) Insect Life Cycle Modeling (ILCYM) software—a new tool for Regional and global insect pest risk assessments under current and future climate change scenarios. CABI Book publication: 412–427.
69. Tonnang EZH, Juarez H, Carhuapoma P, Gonzales JC, Mendoza D, Sporleder M, Simon R, Kroschel J (2013) ILCYM—Insect Life Cycle Modeling. A software package for developing temperature-based insect phenology models with applications for local, regional and global analysis of insect population and mapping. Lima, Peru, International Potato Center Pp. 193.
70. Khadioli N, Tonnang ZEH, Muchugu E, Ongamo G, Achia T, Kipchirchir I, Kroschel J, Le Ru B (2014) Effect of temperature on the phenology of *Chilo partellus* (Swinhoe) (Lepidoptera, Crambidae): simulation and visualization of the potential future distribution of *C. partellus* in Africa under warmer temperatures through the development of life-table parameters. *Bull Entomol Res* 104: 809–822. <https://doi.org/10.1017/S0007485314000601> PMID: 25229840
71. Akaike H (1973) Information theory as an extension of the maximum likelihood principle. pp. 267–281 in Petrov, B.N. & Csaki, K. (Eds) Second International Symposium on Information Theory. Akademiai Kiado, Budapest.
72. Taylor F (1981) Ecology and evolution of physiological time in insects. *Am Nat* 117: 1–23.
73. QGIS Development Team (2009). QGIS Geographic Information System. Open Source Geospatial Foundation. <http://qgis.osgeo.org>. Accessed 17th June 2016.
74. American National Standards Institute (2007). American National Standard for Information Systems-Coded Character Sets—7-Bit American National Standard Code for Information Interchange (7-Bit ASCII). ANSI INCITS 4–1986. <http://sliderule.mraio.com/w/images/7/73/ASCII.pdf>. Accessed 08th December 2016.
75. Mwatawala M, Virgilio M, Joseph J, De Meyer M (2015) Niche partitioning among two *Ceratitis rosa* morphotypes and other Ceratitis pest species (Diptera, Tephritidae) along an altitudinal transect in Central Tanzania. In: De Meyer M, Clarke AR, Vera MT, Hendrichs J (Eds) Resolution of Cryptic Species Complexes of Tephritis Pests to Enhance SIT Application and Facilitate International Trade. *ZooKeys* 540: 429–442. <https://doi.org/10.3897/zookeys.540.6016> PMID: 26798271
76. Nyamukondwa C, Kleynhans E, Terblanche JS (2010) Phenotypic plasticity of thermal tolerance contributes to the invasion potential of Mediterranean fruit flies (*Ceratitis capitata*). *Ecol. Entomol.* 35:565–575.
77. Salum J, Mwatawala K., M., Kusolwa P., and De Meyer M. (2013) Demographic parameters of the two main fruit fly (Diptera Tephritidae) species attacking mango in Central Tanzania. *J. Appl. Entomol* 138: 441–448.
78. Vargas R. I., Walsh W. A., Kanehisa D., Stark J. D., and Nishida T. (2000) Comparative demography of three Hawaiian fruit flies (Diptera: Tephritidae) at alternating temperatures. *Ann Entomol Soc Amer* 93: 75–81.
79. Stevens GC (1989) The latitudinal gradient and geographical range: how so many species coexist in the tropics. *The American Naturalist* 133, 240–250. Stinner RE, Butler GD, Bachelet JS, Tuttle C, 1975. Simulation of temperature-dependent development in population dynamics models. *Can Entomol* 107 (11): 1167–1174.

80. Copeland RS, Wharton RA, Luke Q, De Meyer M, Lux S, Zenz N, Machera P, Okumu M (2006) Geographic distribution, host fruit, and parasitoids of African fruit fly pests *Ceratitis anoneae*, *Ceratitis cosyra*, *Ceratitis fasciventris*, and *Ceratitis rosa* (Diptera: Tephritidae) in Kenya. Ann Entomol Soc Am 99(2): 261–78.
81. De Villiers M, Manrakhan A, Addison P, Hattingh V (2013) The distribution, relative abundance, and seasonal phenology of *Ceratitis capitata*, *Ceratitis rosa*, and *Ceratitis cosyra* (Diptera: Tephritidae) in South Africa. Environ Entomol 42: 831–840. <https://doi.org/10.1603/EN12289> PMID: 24331596
82. Ye H. & Liu (2007) Population dynamics of oriental fruit fly *Bactrocera dorsalis* (Diptera: Tephritidae) in Xishuangbanna, Yunnan Province, China. J Front Agric China 1: 76.
83. Broufas G. D., Pappas M. L., and Koveos D. S. (2009) Effect of Relative Humidity on Longevity, Ovarian Maturation, and Egg Production in the Olive Fruit Fly (Diptera: Tephritidae). Ann Entomol Soc Amer 102(1):70–75.
84. Aluja M, Norrbom A (1999) Fruit flies (Tephritidae) phylogeny and evolution of behavior. CRC Press, Boca Raton 967 pp.
85. Ricalde MP, Nava DE, Loeck AE, Donatti MG (2012) Temperature-dependent development and survival of Brazilian populations of the Mediterranean fruit fly, *Ceratitis capitata*, from tropical, subtropical and temperate regions. J Insect Sci 12: 33. <https://doi.org/10.1673/031.012.3301> PMID: 22963468
86. Meirelles RN, Redaelli LR, Ourique CB (2015) Thermal Requirements and Annual Number of Generations of *Diachasmimorpha longicaudata* (Hymenoptera: Braconidae) Reared in the South American Fruit Fly and the Mediterranean fruit fly (Diptera: Tephritidae). Fla Entomol 98(4): 1223–1226.
87. De Meyer M, Copeland RS, Lux S, Mansell M, Wharton R, White IM, Zenz N (2002) Annotated check list of host plants for Afrotropical fruit flies (Diptera: Tephritidae) of the genus *Ceratitis*. Zoologische Documentatie Koninklijk Museum voor Midden Afrika 27: 1–92.
88. Weldon CW, Boardman L, Marlin D, Terblanche JS (2016) Physiological mechanisms of dehydration tolerance contribute to the invasion potential of *Ceratitis capitata* (Wiedemann) (Diptera: Tephritidae) relative to its less widely distributed congeners. Front. Zool 13:15. <https://doi.org/10.1186/s12983-016-0147-z> PMID: 27034703
89. Diamantidis AD, Carey JR, Nakas CT, Papadopoulos NT (2011a) Ancestral populations perform better in a novel environment: domestication of five medfly populations from five global regions. Biol. J. Linnean Soc. 102:334–345.
90. Diamantidis AD, Carey JR, Nakas CT, Papadopoulos NT (2011b) Population-specific demography and invasion potential in medfly. Ecol Evol. 1: 479–488. <https://doi.org/10.1002/ece3.33> PMID: 22393516